



Deposited via The University of Leeds.

White Rose Research Online URL for this paper:

<https://eprints.whiterose.ac.uk/id/eprint/88994/>

Version: Accepted Version

---

**Article:**

Pei, Y, Paton, DA, Knipe, RJ et al. (2015) A Review Of Fault Sealing Behaviour And Its Evaluation In Siliciclastic Rocks. *Earth-Science Reviews*, 150. 121 - 138. ISSN: 0012-8252

<https://doi.org/10.1016/j.earscirev.2015.07.011>

---

© 2015, Elsevier. Licensed under the Creative Commons Attribution-NonCommercial-NoDerivatives 4.0 International <http://creativecommons.org/licenses/by-nc-nd/4.0/>

**Reuse**

Items deposited in White Rose Research Online are protected by copyright, with all rights reserved unless indicated otherwise. They may be downloaded and/or printed for private study, or other acts as permitted by national copyright laws. The publisher or other rights holders may allow further reproduction and re-use of the full text version. This is indicated by the licence information on the White Rose Research Online record for the item.

**Takedown**

If you consider content in White Rose Research Online to be in breach of UK law, please notify us by emailing [eprints@whiterose.ac.uk](mailto:eprints@whiterose.ac.uk) including the URL of the record and the reason for the withdrawal request.



24 effects of stratigraphic juxtaposition between hanging wall and footwall on  
25 the sealing properties of a fault zone. The study on the detailed fault zone  
26 architecture also implies the importance of fault arrays that increase the  
27 complexity of overall stratigraphic juxtaposition between hanging wall and  
28 footwall. The fault seal processes and their generated fault rocks play an  
29 important control on sealing properties of a fault zone. Temperature and  
30 stress history, which are closely related to burial history, are also found to  
31 control the sealing capacity of a fault zone to some extent. The methods  
32 such as stratigraphic juxtaposition, clay smear indices, microstructural  
33 analysis and petrophysical assessment has significantly boosted the  
34 research of fault sealing behaviour. However, further research is still needed  
35 to increase the effectiveness of present fault seal analysis.

36 **Keywords:** fault zone architecture, fault seal process, fault rocks,  
37 hydrocarbon sealing behaviour

## 38 **1. Introduction**

39 In petroleum exploration and production, as faults can behave as i) conduits,  
40 ii) barriers or iii) combined barrier-conduit structures for hydrocarbon  
41 migration, the presence of faults increases the risks for hydrocarbon drilling,  
42 exploration and development. In order to avoid or minimise the risks, the  
43 way in which faults and fractures affect the hydrocarbon migration has  
44 attracted the interest of geologists. Previous research (e.g., Allan, 1989;  
45 Bouvier et al., 1989; Schowalter, 1979; Smith, 1966; Smith, 1980; Watts,  
46 1987) has studied the fault behaviour and proposed many fundamental  
47 principles that control the fault sealing properties within oil/gas reservoirs. In  
48 the recent 20 years, the abundance of data, including seismic reflection data,

49 structural and micro-structural analysis from both core and field rock  
50 samples, wellbore and production data of oil/gas fields, makes it possible to  
51 conduct fault seal analysis to predict fault-sealing properties.

52 The progress in understanding the faulting processes (Balsamo et al., 2010;  
53 Caine et al., 1996; Childs et al., 2009; Childs et al., 1996b; Walsh et al.,  
54 2003), the fault rock development (Fisher and Knipe, 1998; Jolley et al.,  
55 2007b; Knipe, 1989; Knipe et al., 1997; Tueckmantel et al., 2010), the fault  
56 geometry (Jolley et al., 2007b; Peacock and Sanderson, 1991; Peacock and  
57 Sanderson, 1992; Peacock and Sanderson, 1994; Walsh et al., 2003) and  
58 the fault population (Billi et al., 2003; Cowie et al., 1996; Cowie and Scholz,  
59 1992; Cowie et al., 1993; Faulkner et al., 2010; Kolyukhin et al., 2010; Walsh  
60 et al., 2003) has provided a platform for improving the accuracy of fault  
61 sealing analysis. The studies on the relationship between different fault  
62 parameters, e.g., fault length, fault displacement and fault thickness, has  
63 significantly promoted the understanding the effect of fault architecture on  
64 fault compartmentalization (Faulkner et al., 2003; Fossen et al., 2007; Torabi  
65 and Berg, 2011). Knipe et al. (1992a; 1992b; 1994), Fisher and Knipe (1998;  
66 2001), Fisher et. al. (2003; 2009) and Jolley et. al. (2007a; 2007b) also  
67 highlighted the importance of the fault zone complexity and the petrophysical  
68 properties of the fault rocks in the evaluation of fault-sealing capacity. Firstly,  
69 the fault zone development can involve strain being accommodated by a  
70 complex array of faults not just a single, through-going fault; secondly, the  
71 sealing capacity of the fault zones may vary significantly depending on the  
72 composition of the host rocks that are entrained into the fault zones. Given  
73 the important control of fault zone complexity and petrophysical properties of

74 the fault rocks, their controlling factors have been considered in recent  
75 studies:

76 i) the changing chemical/physical processes with time, e.g., the  
77 burial/temperature history (Fisher et al., 2003; Fossen et al., 2007; Jolley et al.,  
78 2007b) and the amount/rate of strain (Balsamo et al., 2010; Faulkner et al.,  
79 2010; Fossen and Bale, 2007);

80 ii) the diagenetic processes that affect the fault sealing capacity, e.g.,  
81 disaggregation, clay/phyllsilicate smearing, cataclasis, pressure solution and  
82 cementation (Faulkner et al., 2010; Fossen et al., 2011; Tueckmantel et al.,  
83 2010).

84 Although geologists have also realized the importance of the fault zone  
85 architecture within carbonates and its sealing properties in recent years  
86 (Agosta et al., 2012; Brogi and Novellino, 2015; Collettini et al., 2014;  
87 Faulkner et al., 2003; Fondriest et al., 2012; Korneva et al., 2014; Rotevatn  
88 and Bastesen, 2014), majority of fault sealing analysis has still focused on  
89 the fault zone architecture and fault seal analysis in siliciclastic reservoirs  
90 since 1980s. Apparently, the studies of fault zone architecture and  
91 hydrocarbon sealing behaviour in siliciclastic reservoirs are more thorough  
92 and therefore this review paper has focused on siliciclastic reservoirs by  
93 integrating the previous studies of different perspectives. In this paper, we  
94 firstly review the sealing behaviour of a fault zone in the aspects of fault  
95 zone architecture, fault seal types, fault seal processes, fault rock  
96 classification, methods and controlling factors; and then discuss the  
97 limitations of the current models/methods to give suggestions on the future  
98 work on fault zone architecture and its effects on hydrocarbon sealing  
99 behaviour.

## 100 **2. Fault Zone Architecture**

101 Understanding the effects of stress on given rock volumes is of importance  
102 to the investigation of rock deformation mechanisms and their effects on  
103 hydrocarbon sealing behaviour of a fault zone. The competent rocks (e.g.  
104 sandstones or carbonates) are inclined to brittle deformation (e.g., faulting),  
105 whereas the incompetent rocks (e.g., mudstones or shales) prefer to ductile  
106 deformation (e.g., folding). In previous studies focusing on the deformation  
107 mechanisms of the mechanically layered sequence, it has been reported  
108 that the faults tend to form first in the brittle beds (e.g. cemented sandstones  
109 or carbonates); while the weak/ductile beds (e.g. clay beds) deform by  
110 distributed shear to accommodate the overall strain ([Childs et al., 1996a](#);  
111 [Eisenstadt and De Paor, 1987](#); [McGrath and Davison, 1995](#); [Peacock and  
112 Sanderson, 1992](#); [Schöpfer et al., 2006](#)). Several quantitative dynamic  
113 models have been presented (e.g., [Egholm et al., 2008](#); [Welch et al., 2009a](#);  
114 [Welch et al., 2009b](#); [Welch et al., 2015](#)) to analyse the mechanics of  
115 clay/shale smearing along faults in layered sand and shale/clay sequences.  
116 These models predict that the isolated initial faults formed within the brittle  
117 beds will grow until eventually they link up with increasing strain, by  
118 propagating across the ductile intervals to create a complex fault zone  
119 architecture ([Childs et al., 1996a](#); [Peacock and Sanderson, 1991](#); [Walsh et  
120 al., 2003](#); [Walsh et al., 1999](#); [Welch et al., 2009a](#); [Welch et al., 2009b](#)). Many  
121 natural examples support those previous studies on detailed fault zone  
122 architecture, e.g., the deformed interbedded sandstones and shales derived  
123 from the Cutler Formation juxtaposed against limestone from the Honaker  
124 Trail Formation near the entrance to Arches National Park ([Davatzes and](#)

125 [Aydin, 2005](#)); the outcrop studies from a minor normal-fault array exposed  
126 within Gulf of Corinth rift sediments, Central Greece ([Loveless et al., 2011](#));  
127 and the multilayer systems in the South-Eastern basin, France ([Roche et al.,](#)  
128 [2012](#)). Fault zone models defining the fault zone architecture have also been  
129 proposed, e.g., the fault zone model in crystalline rocks ([Caine et al., 1996](#));  
130 the fault zone model in poorly lithified sediments ([Heynekamp et al., 1999](#);  
131 [Rawling and Goodwin, 2003](#); [Rawling and Goodwin, 2006](#)); and the dynamic  
132 fault zone models within poorly consolidated sediments by [Balsamo et. al.](#)  
133 ([2010](#)) and [Loveless et al. \(2011\)](#).

134 As reviewed by [Knipe et. al. \(1997; 1998\)](#), fault zone geometry and fault  
135 population play an important control on the fluid flow properties of fault  
136 zones. The internal structures of individual fault zones need to be  
137 considered because it affects the distribution of fault rocks and stratigraphic  
138 juxtaposition (e.g., [Faulkner et al., 2010](#); [Rawling et al., 2001](#); [Walsh et al.,](#)  
139 [1998](#); [Yielding et al., 1996](#)). For example, in the fault core and damage zone  
140 model of [Caine et. al. \(1996\)](#), the fault core was taken as a barrier and the  
141 damage zone was taken as a conduit for cross-fault fluid flow (Fig.1a);  
142 however, [Faulkner et. al. \(2010; 2003\)](#) found that the intricate internal  
143 structures of a fault zone can potentially lead to high degree of permeability  
144 heterogeneity and anisotropy (Fig.1b). Many case studies have supported  
145 these results, e.g., the fault zone structure and slip localization ([Choi et al.,](#)  
146 [2015](#); [Collettini et al., 2014](#); [Fondriest et al., 2012](#)), the fluid flow properties  
147 of a relay zones ([Fachri et al., 2013a](#); [Qu et al., 2015](#); [Rotevatn et al., 2007](#)),  
148 etc.

149 Fig.1 Typical fault zone structures (Faulkner et al., 2010). (a) Shows a single  
150 high-strain core surrounded by a fractured damage zone (Caine et al.,  
151 1996) and (b) shows multiple cores model, where many strands of  
152 high-strain material enclose fractured lenses (Faulkner et al., 2003).  
153 The diagrams of fracture density and permeability indicate that the  
154 complexity of fault zone geometry and fault population can play  
155 important control on the fluid flow properties.

### 156 3. Fault seal types

157 Although there have not been universal agreements reached on the fault  
158 seal classifications, two types of fault seals have already been recognized,  
159 which are juxtaposition seals and fault rock seals (e.g., Cervený et al., 2004;  
160 Faulkner et al., 2010; Jolley et al., 2007a; Jones and Hillis, 2003; Knipe,  
161 1992a; Knipe et al., 1997; Knott, 1993).

#### 162 3.1. Juxtaposition seals

163 Juxtaposition seals are associated with cases where cross fault juxtaposition  
164 with low permeability non-reservoir units occurs and have been well  
165 described in previous studies (Allan, 1989; Knipe, 1997). When a sequence  
166 of beds is cut by faults, the hanging wall can be considered to move  
167 downward for normal faults; upward for thrust faults; and laterally for strike  
168 slip faults. The relative movement between the two walls of the faults gives  
169 rise to the occurrence of juxtaposition between the rocks with different  
170 lithology or petrophysical properties in the hanging wall and the footwall. As  
171 rocks with different lithology usually have different petrophysical properties  
172 (e.g. different porosity, permeability, capillary entry pressure), there will be a  
173 permeability gradient between different rocks juxtaposed between the

174 hanging wall and the footwall. Juxtaposition seals between the hanging wall  
175 and the footwall can be produced by this process. For instance, it is possible  
176 to form juxtaposition seals when a sandstone bed is juxtaposed with a  
177 mudstone/shale bed; in contrast, it may not form a juxtaposition seal when a  
178 sandstone bed juxtaposes with a sandstone bed.

179 Fig.2 is a schematic diagram demonstrating the occurrence of the  
180 juxtaposition seals. As the hanging wall moves downward relative to the  
181 footwall, different stratigraphic units (A: mudstone; B: sandstone; C:  
182 mudstone) from the hanging wall and the footwall juxtapose against each  
183 other. For example, the mudstone bed (A) of the hanging wall juxtaposes  
184 against the sandstone bed (B) of the footwall (polygon I); B of the hanging  
185 wall juxtaposes against B of the footwall (polygon II); and B of the hanging  
186 wall juxtaposes against C of the footwall (polygon III). As sandstone  
187 presents higher permeability and lower capillary entry pressure than  
188 mudstone, the juxtaposition seals can happen in polygon I and polygon III,  
189 but do not happen in polygon II. Apart from the lithology of the hanging wall  
190 and footwall, the layer thickness and fault throw are also of importance to  
191 juxtaposition seals. For a permeable layer (e.g., sandstones) with a certain  
192 thickness, the permeable layers can be self-juxtaposed to form conduits for  
193 hydrocarbon migration if the fault throw was smaller than the thickness,  
194 whereas juxtaposition seals may occur if the fault throw exceeded the  
195 thickness. For a certain fault throw, a permeable layer thicker than the fault  
196 throw can be self-juxtaposed to form conduits for hydrocarbon migration,  
197 whereas a permeable layer thinner than the fault throw can possibly  
198 generate juxtaposition seals.

199 Fig.2 A schematic diagram shows stratigraphic juxtaposition between the  
200 hanging wall and footwall (modified from Knipe et al., 1997).  
201 Juxtaposition seal can occur when low-permeable rocks in the hanging  
202 wall juxtapose against high-permeable rocks in the footwall (e.g.,  
203 polygon I and III).

### 204 **3.2. Fault rock seals**

205 According to terminology for structural discontinuities reviewed by Schultz  
206 and Fossen (2008), the term 'fault' is defined as a single plane that has been  
207 called a slip plane or shear fracture, whereas the term 'fault zone' is a  
208 tabular region containing a set of parallel or anastomosing fault surfaces. As  
209 shown in natural examples (e.g., Fig.1), many faults are not single-plane  
210 faults but composed of a series of fault planes or networks of small fault  
211 segments that form fault zones (Caine et al., 1996; Childs et al., 1996a;  
212 Childs et al., 1996b; Faulkner et al., 2010; Knipe et al., 1997). Different fault  
213 rocks are then generated when different types of host rocks are entrained  
214 into the complex fault zones during faulting (Fisher and Knipe, 1998; Fossen  
215 et al., 2007; Knipe et al., 1997; Knipe et al., 1998; Manzocchi et al., 2010;  
216 Ottesen Ellevset et al., 1998). The study of Watts (1987) highlighted that  
217 most faults/fault zones were membranes or flow retarders with different  
218 properties of transmissibility or permeability. As the sealing properties of  
219 fault rocks can be evaluated by the permeability and the capillary threshold  
220 pressure (Fisher and Jolley, 2007; Fisher and Knipe, 2001; Watts, 1987), the  
221 fluid flow across the fault zones will not happen unless the capillary  
222 threshold pressure is reached. Therefore, the petrophysical properties of the

223 fault rocks, such as the capillary threshold pressure and permeability control  
224 the hydrocarbon sealing properties of faults/fault zones.

225 As pointed out (Fisher and Knipe, 1998; Knipe et al., 1997), the composition  
226 of the host sediments at the time of deformation determines the deformation  
227 mechanisms, microstructures and petrophysical properties of the fault rocks  
228 within the fault zones; and therefore fault rock seals may occur if fault rocks  
229 with low permeability and high capillary threshold pressure are generated  
230 within the fault zones.

#### 231 **4. Fault Seal Processes**

232 The fundamental fault seal processes that give rise to the occurrence of fault  
233 related permeability barriers have been studied in detail in the past 30 years  
234 (e.g., Fisher et al., 2003; Fisher and Knipe, 1998; Fisher et al., 2009; Fossen  
235 and Bale, 2007; Fossen et al., 2007; Fossen et al., 2011; Knipe, 1989; Knipe,  
236 1992a; Knipe, 1993a; Knipe, 1993b; Knipe et al., 1998; Tueckmantel et al.,  
237 2010). Five types of fault seal processes have been identified, which are: (i)  
238 clay/phyllosilicate smearing; (ii) cementation; (iii) cataclasis; (iv) diffusive  
239 mass transfer by pressure solution or quartz cementation; and (v) porosity  
240 reduction by disaggregation or mixing. However, as Knipe (1997) pointed out,  
241 these five fault seal processes can either perform individually during  
242 deformation or combine interactively with each other.

##### 243 **4.1. Clay/Phyllosilicate Smearing**

244 As continuous clay/phyllosilicate smear has very low porosity and  
245 permeability (Smith, 1966; Smith, 1980), it acts as an extremely effective  
246 fluid flow barrier and therefore many studies have focused on this fault seal  
247 process. For example, deformation induced shearing of clays/phyllosilicates

248 has been discussed in previous studies (e.g., Aydin and Eyal, 2002; Bouvier  
249 et al., 1989; Fulljames et al., 1997; Gibson, 1994; Yielding et al., 1997).

250 Three principle means of clay/phyllosilicate smearing are proposed by  
251 Lindsay et al. (1993), which are:

- 252 a). abrasion of clay/phyllosilicate when it is moving past sandstones;
- 253 b). shearing and ductile deformation of beds (with high clay/phyllosilicate  
254 content, e.g. shale or mudstone beds) between hanging wall and footwall;
- 255 c). injection of clay/phyllosilicate materials during fluidisation.

256 It is suggested that the continuity of clay/phyllosilicate smearing is  
257 determined by a series of parameters including the sedimentary lithification  
258 state, the effective stress, the confining pressure, the strain rate and the  
259 mineralogy (Fisher and Knipe, 1998).

260 Several algorithms have been proposed to evaluate the fault sealing  
261 properties quantitatively, either based on the continuity of clay/phyllosilicate  
262 smears or average clay content within the fault zones, e.g., Clay Smear  
263 Potential (CSP) (Bouvier et al., 1989; Fulljames et al., 1997), Shale Smear  
264 Factor (SSF) (Lindsay et al., 1993), Shale Gouge Ratio (SGR) (Yielding et  
265 al., 1997) and Scaled Shale Gouge Ratio (SSGR) (Ciftci et al., 2013). These  
266 algorithms evaluate the fault sealing properties by considering the re-  
267 distribution of mudstone/shale beds or the clay/phyllosilicate content of the  
268 beds in sheared fractures. Empirically, the stacking sequences with high  
269 clay/phyllosilicate content are likely to form fault zones with low permeability.  
270 During the deformation of fault rocks, there can be two competing  
271 compaction mechanisms which are the mechanical compaction and  
272 chemical compaction (Fisher and Knipe, 2001). These two compaction

273 mechanisms affect fault rock properties depending on the clay/phyllsilicate  
274 content of the host rocks. For example, faults developed in impure  
275 sandstones (clay content of 15-25%) experienced enhanced chemical  
276 compaction (e.g., grain-contact quartz dissolution), whereas faults in clay-  
277 rich sandstones (clay content of >25%) are dominated by mechanical  
278 compaction. The higher clay/phyllsilicate content in host rocks can  
279 significantly decrease the effective quartz surface area, which lead to the  
280 inhibition of the chemical compaction (e.g., quartz cementation) (Fisher and  
281 Knipe, 1998). The competition between the two mechanisms results in the  
282 relationship between clay/phyllsilicate content and fault sealing properties  
283 (e.g., porosity, permeability, capillary pressure) being highly complicated and  
284 can even lack correlation. Therefore, the algorithms, such as CSP (Bouvier  
285 et al., 1989; Fulljames et al., 1997), SSF (Lindsay et al., 1993), SGR  
286 (Yielding et al., 1997) and SSGR (Ciftci et al., 2013), should be used with  
287 caution when evaluating the fluid flow properties of the fault zones.

#### 288 **4.2. Cementation**

289 The most common result of deformation related cementation includes  
290 cemented faults or fractures (Fisher and Knipe, 1998; Fisher and Knipe,  
291 2001; Fisher et al., 2009; Fossen and Bale, 2007; Fossen et al., 2011;  
292 Tueckmantel et al., 2010). The microstructures of these features provide  
293 important evidence for studying the mechanisms and timing of the  
294 cementation processes. As faults/fractures may perform as conduits for fluid  
295 flow, the flow behaviour of faults/fractures is sensitive to quartz precipitation  
296 because within the fault zones there are both quartz sources (from  
297 dissolution) and nucleation sites for potential cementation. The source for

298 cementation can be internal or external, but [Fisher and Knipe \(1998\)](#) pointed  
299 out that natural oil/gas field examples do not always require that an external  
300 fluid source controls the sealing properties of the fault zones, especially at a  
301 large scale where the external fluids may not promote continuous  
302 cementation for extensive sealing.

303 As there may be impure sandstones containing clay minerals, it is important  
304 to understand the effects of clay minerals on the quartz cementation, which  
305 has been well established in previous studies (e.g., [Bjorkum, 1996](#); [Dewers  
306 and Ortoleva, 1991](#); [Fisher and Knipe, 1998](#); [Fisher and Knipe, 2001](#);  
307 [Fossen and Bale, 2007](#); [Fossen et al., 2011](#); [Heald, 1955](#); [Oelkers et al.,  
308 1996](#)). It is suggested that small concentrations of clay/phyllosilicate  
309 minerals in sandstones increase the potential of cementation as the  
310 clay/phyllosilicate minerals can act as a local source for cementation  
311 ([Dewers and Ortoleva, 1991](#); [Fisher et al., 2003](#); [Fisher et al., 2009](#); [Heald,  
312 1955](#); [Knipe, 1993a](#); [Oelkers et al., 1996](#)). However, high clay/phyllosilicate  
313 contents can lead to the clay/phyllosilicate-coating on the quartz grains,  
314 which decreases the effective quartz grain surface area available for  
315 cementation ([Cecil and Heald, 1971](#); [Fisher et al., 2003](#); [Fossen and Bale,  
316 2007](#); [Fossen et al., 2011](#); [Tada and Siever, 1989](#); [Walderhaug, 1996](#)).

### 317 **4.3. Cataclasis**

318 Cataclasis involves grain fracturing and can reduce the porosity and the  
319 permeability as well as increase the capillary threshold pressure of rocks  
320 within fault zones (e.g., [Antonellini and Aydin, 1994](#); [Antonellini and Aydin,  
321 1995](#); [Borg et al., 1960](#); [Engelder, 1974](#); [Knipe, 1989](#)). During the process of  
322 cataclasis, the porosity and permeability are reduced because the cataclasis

323 results in the collapse of porosity and the reduction of grain size (Fisher and  
324 Knipe, 1998). Rawling and Goodwin (2003) also suggests that cataclasis  
325 presents different micro-deformation mechanisms depending on the burial  
326 depth, i.e., cataclasis in sediments at shallow depths is dominated by grain  
327 spalling and flaking whereas cataclasis at deeper depths is primarily  
328 characterized by transgranular fracturing and grain crushing. The grain-  
329 sorting within cataclasites is becoming poorer by grain fracturing and  
330 chipping at early stage, and the following predominant chipping and crushing  
331 then enhance the grain sorting. As an effective tool to study the cataclasis  
332 processes of fault rocks, micro-structural analysis has been utilized in many  
333 case studies (Antonellini et al., 1994; Blenkinsop, 1991; Fisher and Knipe,  
334 1998; Jolley et al., 2007b; Tueckmantel et al., 2010), suggesting that the  
335 concentration of clay/phyllosilicate materials in host rocks can inhibit the  
336 probability of occurrence of cataclasis. Therefore, the sandstones with high  
337 clay/phyllosilicate content are likely to be resistant to the cataclasis during  
338 faulting deformation, as the clay/phyllosilicate-rich sandstones tend to  
339 deform more easily by grain sliding and rotation rather than by grain  
340 fracturing. However, different textures of impure sandstones (e.g., the  
341 distribution of clay/phyllosilicate minerals) also affect the modalities of  
342 cataclastic deformation.

#### 343 **4.4. Diffusive Mass Transfer by Pressure Solution and Quartz**

##### 344 **Cementation**

345 Diffusive mass transfer, a process of mass transfer from high-pressure sites  
346 to low-pressure sites, happens when materials are dissolved at the grain  
347 contacts and then transported by diffusion to free pore spaces where the

348 dissolved materials reprecipitate (Fisher and Knipe, 1998; Fisher et al., 2009;  
349 Fossen et al., 2007; Knipe et al., 1997; Rutter, 1983; Spiers and Schutjens,  
350 1990). Diffusive mass transfer is actually a redistribution of soluble materials  
351 from their original sites with high pressure, by means of dissolution, transport  
352 and reprecipitation (Dewers and Ortoleva, 1990; Fisher et al., 2009; Knipe et  
353 al., 1997; Tueckmantel et al., 2010); and can alter the porosity and  
354 permeability of fault rocks.

355 Based on the micro-structural analysis, it is found that the extent of diffusive  
356 mass transfer is dominated by the clay/phyllsilicate content and its  
357 distribution at the time of deformation (Fisher and Knipe (1998); Fisher and  
358 Knipe, 2001; Fossen et al., 2007; Tueckmantel et al., 2010). For example: (i).  
359 for clean sandstones with clay/phyllsilicate contents of <5%, the fault zones  
360 experience enhanced quartz cementation within fault zones but can occur  
361 with no enhanced pressure solution (i.e. an external source is involved); (ii).  
362 for clean sandstones with higher clay/phyllsilicate content of 5-15%, there  
363 is evidence for both enhanced pressure solution and quartz cementation (i.e.  
364 an internal source is involved); (iii). for impure sandstones with  
365 clay/phyllsilicate contents of 15-25%, the fault zones can experience  
366 enhanced pressure solution but no extensive enhanced quartz cementation;  
367 (iv). for impure sandstones with clay/phyllsilicate content of >25%, the  
368 porosity and permeability of the fault zones may not be significantly affected  
369 by either pressure solution or quartz cementation. The reason for these  
370 observations is that diffusive mass transfer needs a catalyst  
371 (clay/phyllsilicate) for pressure solution as well as nucleation sites for  
372 quartz cementation. The rate of diffusive mass transfer is especially

373 determined by the presence and distribution of clay/phyllsilicate. For  
374 example, the presence of small concentration of clay/phyllsilicate minerals  
375 at the grain-contact points promotes the occurrence of pressure solution (e.g.  
376 Odling et al., 2004); while clay/phyllsilicate-coating on the quartz grains  
377 inhibits the quartz cementation (e.g. Tada and Siever, 1989), because the  
378 coating clay/phyllsilicate minerals reduce the effective surface area of  
379 quartz grains available for precipitation.

#### 380 **4.5. Porosity Reduction by Disaggregation and Mixing**

381 In this fault seal process, there is no extensive grain fracturing but just  
382 disaggregation and mixing of grains by means of particulate flow (Rawling  
383 and Goodwin, 2003; Rawling and Goodwin, 2006), e.g., grain rolling and  
384 grain sliding, which means this process results in the reorganisation of  
385 distribution of detrital grains and clay/phyllsilicate minerals without a  
386 universal reduction of grain size (Fisher and Knipe, 1998; Fossen et al.,  
387 2007; Knipe et al., 1997; Ottesen Ellevset et al., 1998). This fault process is  
388 common in sedimentary units that are unconsolidated or unlithified, as in this  
389 situation there is enough space for grains and clay/phyllsilicate minerals to  
390 be redistributed during faulting deformation (Bense et al., 2003; Fisher and  
391 Knipe, 1998; Fossen et al., 2007; Knipe et al., 1997; Ottesen Ellevset et al.,  
392 1998). The sedimentary units that are buried at shallow depths tend to  
393 experience disaggregation and mixing to reduce the rock porosity. The  
394 distribution of both detrital grains and clay/phyllsilicate minerals can be  
395 heterogeneous when initially deposited and then becomes more  
396 homogeneous after the disaggregation and mixing during faulting  
397 deformation, thus altering permeability pathways.

398 The permeability of fault rocks produced by disaggregation and mixing  
399 varies within a big range, depending on the clay/phyllsilicate content of the  
400 host rocks (Fisher and Knipe, 1998; Knipe et al., 1997). Furthermore, it is  
401 suggested that disaggregation can result in either an enhancement or a  
402 reduction of porosity, which depends on whether the disaggregation zone  
403 has a dilational or compactional component (Fossen and Bale, 2007; Fossen  
404 et al., 2007; Fossen et al., 2011). For clean sandstones, because the grain  
405 size and grain sorting of the fault rock do not change considerably after the  
406 reorganization of detrital grains, the fault rock porosity and permeability are  
407 not changed significantly. In contrast, for impure sandstones, as well as the  
408 reorganization of detrital grains, the fine-grained clay/phyllsilicate minerals  
409 are also mixed with these detrital grains, resulting in the occupation of micro-  
410 porosity between the detrital grains by the fine-grained clay/phyllsilicate  
411 minerals. In this scenario, barriers for fluid flow can be produced and the  
412 sealing capacity is effectively increased. Although Fisher and Knipe  
413 observed a permeability reduction of up to one order of magnitude in  
414 phyllsilicate-bearing disaggregation zones (Fisher and Knipe, 2001),  
415 disaggregation zones generally have very limited effects on the permeability  
416 of sandstone reservoirs as the permeability contrast is relatively low (Fossen  
417 et al., 2007).

## 418 **5. Fault rock classification**

419 Fisher and Knipe (2001) suggested that fluid flow properties of faults are  
420 significantly influenced by the presence of clay/phyllsilicate in three ways:  
421 (i). the high concentrations of clay/phyllsilicate can produce fault rocks  
422 within which most of the original porosity is occupied by the fine grained

423 clay/phylosilicate minerals and the micro-porosity (Fisher and Knipe, 1998);  
424 (ii). there is a higher potential for clay/phylosilicate smearing within the  
425 sedimentary units with high clay/phylosilicate contents (Lindsay et al., 1993);  
426 and (iii). the existence of clay/phylosilicate materials between framework-  
427 silicate grains promotes pressure solution and quartz cementation (Fisher  
428 and Knipe, 1998). Therefore, if the faults maintain self-juxtaposition of these  
429 units, the fault rock types related to the fault rock seals can be classified  
430 according to the composition (especially the clay/phylosilicate content) of  
431 the host rocks from which the fault rocks are produced. Where faulting  
432 exceeds the thickness of the host units, the resulting clay content of the fault  
433 rock (from smearing and mixing of the host rocks involved in the faulting),  
434 grain size reduction processes and the potential for cementation can impact  
435 on the fault rock flow properties.

436 Fault rocks can therefore be classified into the following groups (Fisher et al.,  
437 2003; Fisher and Knipe, 1998; Fisher et al., 2009; Knipe et al., 1997;  
438 Ottesen Ellevset et al., 1998): the cemented faults/fractures; the  
439 clay/phylosilicate smears; the phyllosilicate-framework fault rocks (PFFRs);  
440 the cataclasites; and the disaggregation zones (Fig.3). This classification is  
441 based on the relationship between the clay/phylosilicate content and fault  
442 rock types.

443 Fig.3 Illustration of typical fault rocks and their clay/phylosilicate contents,  
444 showing the important control of the clay/phylosilicate content on the  
445 fault rock development (modified from Ottesen Ellevset et al., 1998).

## 446 5.1. Cemented faults/fractures

447 Fault seal analysis based on the prediction of fault rock clay contents can be  
448 invalidated if cemented fault zones are extensively developed (Fig.4) (Jolley  
449 et al., 2007b; Knipe, 1993a; Knipe et al., 1997). However, in most cases, the  
450 cementation is not extensive enough to influence the sealing properties of  
451 the fault zones (Ottesen Ellevset et al., 1998), as the cementation can rarely  
452 form continuous seals but is often restricted to limited areas of the fault zone  
453 or between the footwall and the hanging wall cut offs of units prone to  
454 cementation.

455 Fig.4 A schematic cartoon (modified from Jolley et al., 2007b) and a typical  
456 micro-graph (Pei, 2013) of cemented faults/fractures. The cement seals  
457 can occur when minerals' dissolution-reprecipitation process or new  
458 minerals' precipitation dominate the sealing properties of  
459 faults/fractures.

460 Generally, cement seals only happen in fault zones where the sealing  
461 properties are dominated by the minerals' dissolution-reprecipitation process  
462 or where new minerals' precipitation is promoted (Knipe, 1997). Therefore,  
463 the cement seals are mostly associated with the sites where local dissolution  
464 and reprecipitation happen during deformation or along the invasion paths of  
465 fluids in the faults. For cemented faults and fractures, Knipe et al. (1997)  
466 found that cementation is the dominant mechanism of porosity reduction  
467 within the fault zones. There are probably two main sources of cements: the  
468 local soluble minerals within the fault zones; and the invaded fluids along the  
469 fault planes. Because of the high density of nucleation sites on the fault  
470 planes, both the local soluble minerals and invaded fluids can be easily

471 precipitated along or adjacent to the fault planes. [Ottesen Ellevset et al.](#)  
472 [\(1998\)](#) suggested that the cementation extent along the fault planes may be  
473 limited to three times the thickness of the unit that acts as a source unit for  
474 the cementation.

## 475 **5.2. Clay/Phyllosilicate Smears**

476 As shown in the fault rock classification (Fig.3), fault rocks with  
477 clay/phyllosilicate contents >40% are defined as clay smears. These can  
478 develop from the deformation of a host shale rock with >40%  
479 clay/phyllosilicate content at the time of deformation ([Jolley et al., 2007b](#);  
480 [Knipe, 1997](#); [Knipe et al., 1997](#); [Ottesen Ellevset et al., 1998](#)). In this  
481 situation, a continuous clay material zone with low-permeability along fault  
482 planes can be produced during the faulting deformation (Fig.5). The factors  
483 controlling the clay/phyllosilicate smear continuity are the content and  
484 distribution of clay/phyllosilicate-rich units, fault throw ([Bouvier et al., 1989](#);  
485 [Fulljames et al., 1997](#); [Lindsay et al., 1993](#); [Yielding et al., 1997](#)), and the  
486 lithification state ([Egholm et al., 2008](#); [Heynekamp et al., 1999](#); [Loveless et](#)  
487 [al., 2011](#)). Based on the studies on the distribution of clay smears in Sleipner  
488 Vest of North Sea ([Knipe, 1997](#); [Ottesen Ellevset et al., 1998](#)), it was  
489 suggested that the clay/phyllosilicate smears often become discontinuous  
490 once the fault throw is larger than three times the thickness of  
491 clay/phyllosilicate-rich stratigraphic units.

492 Fig.5 A schematic cartoon ([modified from Jolley et al., 2007b](#)) and a typical  
493 micro-graph ([Pei, 2013](#)) of clay/phyllsilicate smears, containing >40%  
494 clay/phyllsilicate minerals. Clay smears can act as effective seals  
495 when continuous clay material zones are produced along fault planes  
496 during the faulting deformation.

### 497 **5.3. Phyllosilicate-framework fault rocks (PFFRs)**

498 As shown in the fault rock classification (Fig.3), phyllosilicate-framework fault  
499 rocks (PFFRs) contain 15-40% clay/phyllsilicate minerals. These can  
500 develop from impure sandstones containing 15-40% clay/phyllsilicate at the  
501 time of deformation or from the mixing of high and low clay content units  
502 ([Fisher and Knipe, 1998](#); [Jolley et al., 2007b](#); [Knipe, 1992a](#); [Knipe et al.,](#)  
503 [1997](#)). An impure sandstone, with a mixture of phyllosilicates and framework  
504 silicates, can produce PFFRs where the petrophysical properties are  
505 dominated by the generation of anastomosing networks of the micro-smears  
506 around the framework fragments or clasts (Fig.6) ([Knipe, 1997](#)). These  
507 micro-smears may have similar properties to the clay smears; thus, as  
508 pointed out by [Knipe \(1992a\)](#), it is not necessary to have clay units for  
509 creating PFFRs if the sealing properties are determined by the continuity  
510 and the structure of deformed phyllosilicates.

511 [Ottesen Ellevset et al. \(1998\)](#) pointed out that the occurrence of PFFRs has  
512 great effects on the sealing behaviour in two areas, which are the area  
513 where the impure sandstones directly juxtapose against the fault zones; and  
514 the area along fault planes between the hanging wall and footwall cut-offs of  
515 impure sandstone units. The latter scenario is to some extent similar to the  
516 behaviour of clay/phyllsilicate smears. The continuity of the PFFRs

517 determines the effectiveness of PFFRs to form effective retarders for fluid  
518 flow (Fisher and Knipe, 1998; Knipe et al., 1997; Ottesen Ellevset et al.,  
519 1998).

520 Fig.6 A schematic cartoon (modified from Jolley et al., 2007b) and a typical  
521 micro-graph (Pei, 2013) of phyllosilicate-framework fault rocks (PFFRs),  
522 containing 15-40% clay/phyllosilicate minerals. The petrophysical  
523 properties of phyllosilicate-framework fault rocks are dominated by the  
524 generation of anastomosing networks of the micro-smears around the  
525 framework fragments or clasts.

#### 526 **5.4. Cataclasites**

527 Cataclasites dominate seal development in clean sandstones containing <15%  
528 clay content at the time of deformation (Fisher and Knipe, 1998; Jolley et al.,  
529 2007b; Knipe et al., 1997; Ottesen Ellevset et al., 1998). Because of the low  
530 clay content within such host rocks, the main mechanisms of porosity and  
531 permeability reduction are the cataclasis and the post-deformation quartz  
532 cementation (Fisher and Knipe, 1998). During the process of cataclasis, the  
533 grain size decreases by means of grain fracturing and frictional grain rolling,  
534 resulting in the porosity reduction and potential cementation (Fig.7). The  
535 frictional grain rolling lead to the irregular grains sub-parallelly aligned to the  
536 shearing direction, which makes the compaction more easily to reduce the  
537 fault rock porosity. The granulation seams or deformation bands, which are  
538 discussed in many studies (Antonellini and Aydin, 1994; Knipe, 1992a; Knipe,  
539 1993a; Knipe, 1993b), are examples of cataclasites.

540 Fig.7 A schematic cartoon (modified from Jolley et al., 2007b) and a typical  
541 micro-graph (Pei, 2013) of cataclasites, containing <15%  
542 clay/phyllsilicate minerals. The grain size reduction of cataclasites is  
543 dominated by grain fracturing and frictional grain sliding, resulting in the  
544 porosity reduction and potential cementation.

545 Previous research has pointed out that the permeability of cataclasites  
546 varies over a large range; this depends on the lithification state of the host  
547 rocks (Fisher and Knipe, 1998; Knipe et al., 1997). According to the  
548 lithification state, the cataclasites can be divided into three types: (i). poorly  
549 lithified cataclasites, which show little or even no compaction or cementation  
550 (post-deformation) and point contacts are maintained between grains; (ii).  
551 partially lithified cataclasites, which have some compaction and cementation;  
552 and (iii). lithified cataclasites, which comprise grains interlocked by post-  
553 deformation dissolution and/or cementation (Knipe, 1992a; Knipe, 1993b;  
554 Knipe et al., 1997).

## 555 **5.5. Disaggregation Zones**

556 The disaggregation zones are fault rocks generated by deformation without  
557 fracturing. They can also be produced from pure, low clay-content (<15%)  
558 sandstones (Fig.3), similar to the generation of the cataclasites (Fisher and  
559 Knipe, 1998; Fossen et al., 2007; Jolley et al., 2007b; Knipe et al., 1997;  
560 Loveless et al., 2011; Ottesen Ellevset et al., 1998; Rawling and Goodwin,  
561 2003). However, the host rocks of disaggregation zones are normally sands  
562 or poorly consolidated sandstones (Bense et al., 2003; Rawling and  
563 Goodwin, 2006). In the process of disaggregation, the grains move by way  
564 of particulate flow (Rawling and Goodwin, 2003) to accommodate the strain

565 during faulting deformation, with no extensive grain fracturing (Fisher and  
566 Knipe, 1998; Knipe et al., 1997). The permeability of disaggregation zones is  
567 usually higher than that of the other types of fault rocks. It is difficult for  
568 disaggregation to form effective seals to prevent fluid flow, because there  
569 are not sufficient clays/phyllosilicates within the disaggregation zones to act  
570 as a source for either the cementation or the clay/phyllosilicate smears  
571 (Fisher and Knipe, 2001; Fossen et al., 2007) (Fig.8).

572 Fig.8 A schematic cartoon (modified from Jolley et al., 2007b) and a typical  
573 micro-graph (Knipe et al., 1997) of disaggregation zones.  
574 Disaggregation zones are developed in poorly lithified rocks containing  
575 <40% clay/phyllosilicate minerals. As there is not sufficient  
576 clays/phyllosilicates, disaggregation zones cannot form effective seals  
577 for fluid flow under normal conditions.

578 Based on this fundamental fault rock classification, Fisher and Knipe (1998)  
579 constructed the relationship between a wide spectrum of fault rocks with  
580 different geological settings, including clay content, degree of fragmentation  
581 and lithification state (Fig.9). This detailed fault rock classification allows  
582 geologists to make basic prediction of fault rock types (siliciclastic rocks, e.g.,  
583 sandstones, siltstones, mudstones and shales) and properties by  
584 considering clay content, degree of fragmentation and lithification state.

585 Fig.9 Diagram showing different types of fault rocks developed in the North  
586 Sea and their relationship to the composition of the host sediment and  
587 the extent of grain-size reduction and post-deformation lithification  
588 experienced (Fisher and Knipe, 1998).

## 589 **6. Methods to evaluate fault sealing properties**

590 In the recent 20 years, geologists have developed and used several  
591 methods to evaluate the fault sealing properties. The i) Allan map, ii) triangle  
592 juxtaposition diagram and iii) clay smear indices can be employed to  
593 evaluate the fluids flow properties for juxtaposition sealing faults, while the  
594 micro-structural analysis and petrophysical assessment can be used to  
595 investigate the fluids flow properties for fault rock sealing faults (Table 1).  
596 The production simulation modelling also has been employed to predict the  
597 petroleum migration and accumulation features, including consideration of  
598 fault zone compartmentalization and its hydrocarbon sealing behaviour (e.g.,  
599 [Fachri et al., 2013b](#); [Fisher and Jolley, 2007](#); [Manzocchi et al., 2002](#);  
600 [Manzocchi et al., 1999](#); [Ottesen Ellevset et al., 1998](#); [Zijlstra et al., 2007](#)).  
601 Although all these methods have their own shortcomings, the methods have  
602 been improved to become more and more effective and useful for evaluation  
603 of the fault sealing properties.

604 Table 1 A summary of the methods to evaluate fault sealing properties for  
605 different fault seal classifications.

### 606 **6.1. Stratigraphic juxtaposition methods**

607 [Allan \(1989\)](#) introduced a model to relate faults to hydrocarbon migration  
608 and entrapment, suggesting the influence of faults on the hydrocarbon  
609 migration and the entrapment is determined by the lithology of juxtaposed  
610 stratigraphic units on different sides of fault and the fault throws between the  
611 hanging wall and the footwall cut-offs. The model provides a 3D overview  
612 and understanding on the architecture of the fault juxtapositions, the

613 stratigraphic units and the fault throws, which can help to understand the  
614 stratigraphic contacts, the fault geometry and the structure/closure style.

615 [Knipe \(1997\)](#) presented an effective technique of triangle juxtaposition  
616 diagram, which can be used to quickly judge what types of fault seals can be  
617 formed based on the resultant stratigraphic juxtapositions between the  
618 hanging wall and footwall (Fig.10). The Fig.10 illustrates the use of sidewall  
619 charts to review the key host rock characteristics. These variables control  
620 the development of fault rocks and seals. This example shows depth plots of  
621 the host rock properties, porosity, permeability, percentage of phyllosilicate  
622 (abbreviated “Phyllo” in the key) laminations present, and the net/gross  
623 ratios.

624 It is known that reservoir stratigraphic units (e.g., permeable sandstones)  
625 juxtaposing against impermeable stratigraphic units (with high concentration  
626 of clay/phyllosilicate materials, e.g., shales/mudstones) probably form fault  
627 seals; while leaking windows are more likely if reservoir sand stratigraphic  
628 units are juxtaposed against each other. By using the triangle juxtaposition  
629 diagram, it is possible to make an initial judgement and prediction of fault  
630 sealing properties, particularly when seeking possible leaking windows.  
631 Moreover, in the triangle juxtaposition diagram, the sidewall charts can also  
632 be attached to provide more details of the stratigraphy, such as the sand  
633 net/gross ratio, the clay/phyllosilicate content, the host rock lithology and the  
634 host rock permeability (e.g., [Cervený et al., 2004](#); [Knipe, 1997](#); [Knipe et al.,](#)  
635 [1997](#)). These details contribute to allow a more reliable assessment and  
636 prediction of sealing properties on the faults. Different types of juxtapositions  
637 between different stratigraphic units can be identified on this diagram; and

638 these different juxtaposition types provide important clues for estimating the  
639 fault sealing properties of different places on the fault plane with various fault  
640 throws.

641 Fig.10 The triangle juxtaposition diagram uses sidewall chart input to identify  
642 the leaking windows and the fault seals resulting from the stratigraphic  
643 juxtapositions between the hanging wall and the footwall (Knipe, 1997).  
644 The juxtaposition diagram key lists the different types of important  
645 juxtapositions that occur on different parts of the fault plane and  
646 contribute to the fluid flow behavior of faults with different throw  
647 magnitudes. Note that the throws associated with the development of  
648 an area of high-permeability sand juxtaposed against high-permeability  
649 sand (red area) can be rapidly identified.

650 A 3D numerical model of fault displacement, proposed by Clarke et al.  
651 (2005), enables the building of geological models to represent the complex  
652 3D geometry and geological properties of a fault, which can be employed to  
653 predict the cross-fault juxtaposition relationships in 3D space. The further  
654 forward modelling of fault development allows a 4D prediction of fault  
655 juxtaposition (with time). The successful application in the Artemis Field  
656 (Southern North Sea, UK) and the Moab Fault (Utah, USA) demonstrates  
657 significant improvements in the 3D and 4D prediction of fault juxtaposition  
658 seals for both a single fault and multiple faults.

## 659 **6.2. Clay smear indices**

660 Bouvier et al. (1989) employed Clay Smear Potential (CSP) to estimate the  
661 potential of occurrence of clay smearing based on studies of three-  
662 dimensional seismic interpretation and fault sealing investigations in Nun

663 River field in Nigeria. The CSP represents the relative amount of clay (e.g.,  
664 mudstones, shales, etc.) that has been smeared from individual shale  
665 source beds at a certain point along a fault plane during faulting deformation.  
666 The CSP was then expressed more explicitly by [Fulljames et al. \(1997\)](#)  
667 (Fig.11a). The CSP represents the total amount of clay/phyllsilicate that  
668 has been smeared from every stratigraphic unit with high clay/phyllsilicate  
669 content along the fault planes. The value of CSP increases with increasing  
670 thickness of shale/mudstone beds and the number of stratigraphic units with  
671 high concentrations of clay/phyllsilicate, and the CSP decreases with  
672 increasing fault throw.

$$\text{CSP} = \sum \frac{(\text{Shale bed thickness})^2}{\text{Distance from source bed}}$$

673 [Lindsay et al. \(1993\)](#) introduced Shale Smear Factor (SSF, Fig.11b) to  
674 estimate the magnitude of fault seals formed by smearing of  
675 clay/phyllsilicate-rich units, e.g., shales and mudstones. The SSF value is  
676 proportional to the fault throws and inversely proportional to the thickness  
677 and the number of source units of clay/phyllsilicate. Using the SSF  
678 algorithm to estimate the extent of clay/phyllsilicate smears, there is  
679 increasing potential to form a continuous clay/phyllsilicate smears with  
680 increasing thickness and number of source unites of clay/phyllsilicate and  
681 decreasing fault throws, and vice versa.

$$\text{SSF} = \frac{\text{Fault throw}}{\text{Shale layer thickness}}$$

682 The Shale Gouge Ratio (SGR, Fig.11c) was proposed ([Yielding et al., 1997](#))  
683 to estimate the clay content in faults from the mixing of units with different  
684 clay contents in the throw interval. This helps evaluate fault seals in more

685 complex stacking sequences. The SGR is proportional to cumulative  
686 thickness of shale beds within a scale of a distance equal to fault throw and  
687 inversely proportional to fault throw.

$$\text{SGR} = \frac{\sum(\text{Shale bed thickness})}{\text{Fault throw}} \times 100\%$$

688 Furthermore, the definition of SGR was extended for a package of  
689 sediments (Fig.11d). In this situation, SGR is considered to be the  
690 percentage of clay present in all units in the throw interval.

$$\text{SGR} = \frac{\sum[(\text{Zone thickness}) \times (\text{Zone clay fraction})]}{\text{Fault throw}} \times 100\%$$

691 The CSP and SSF estimate the fault sealing properties by considering the  
692 continuity of smearing of shale/mudstone beds; while the SGR calculates the  
693 average mixture of clays likely to be present at different point on a fault.

694 Fig.11 Diagram and calculation of methods for estimation of fault seals  
695 (especially fault seals formed by clay/phyllsilicate smearing): (a) Clay  
696 Smear Potential (CSP) ([Bouvier et al., 1989](#); [Fulljames et al., 1997](#)); (b)  
697 Shale Smear Factor (SSF) ([Lindsay et al., 1993](#)); (c, d) Shale Gouge  
698 Ratio (SGR) ([Yielding et al., 1997](#)).

### 699 **6.3. Microstructural analysis**

700 As introduced above, the fault rocks are generated when the sedimentary  
701 units are entrained into the fault zones. The detailed evaluation of different  
702 types of fault rocks can be achieved by integrating micro-structural analysis  
703 on the deformation mechanisms and the porosity and permeability data. The  
704 Scanning Electron Microscope (SEM) was employed in [Knipe \(1992a\)](#) to  
705 investigate the micro-structures of fault rocks. The following studies ([e.g.](#),

706 Fisher et al., 2003; Fisher and Knipe, 1998; Fisher and Knipe, 2001; Fisher  
707 et al., 2009; Ottesen Ellevset et al., 1998; Rawling and Goodwin, 2003;  
708 Tueckmantel et al., 2010) integrated the fault rock petrophysical sealing  
709 properties with the micro-structural analysis on the fault rocks developed  
710 within the fault zones.

711 Fig.12 The sample photo and BSE micrographs showing the PFFRs  
712 developed in impure sandstones (Pei, 2013).

713 The micro-structural analyses undertaken are laboratory based that aim to  
714 characterise the microstructures and the petrophysical properties of fault  
715 rocks and compare these to their host rocks, in order to estimate the  
716 deformation mechanisms and the fault seal processes that the fault rocks  
717 experienced, and to identify the relative timing of deformation during  
718 diagenesis. For example, Fig.12 presents the BSE micrographs of a fault  
719 rock sample from northern Qaidam basin in China (Pei, 2013). The sample  
720 is located within the fault zone of the fault outcrop, comprising fine-grained  
721 impure sandstone (7-13% clay content) as the dominated lithology. A series  
722 of PFFRs (20-35% clay content) are formed in the shear zones or  
723 deformation bands. The grain size experiences small reduction in the fault  
724 rocks. The BSE micrographs demonstrate the relative high content of fine-  
725 grained phyllosilicates, strong pressure solution and low porosity in the fault  
726 rocks when compared to the surrounding host rocks.

#### 727 **6.4. Petrophysical assessment**

728 The petrophysical properties of the fault rocks have been measured to  
729 evaluate the sealing capacity of the fault rocks quantitatively in many  
730 previous studies (e.g., Fisher and Knipe, 1998; Fisher and Knipe, 2001;

731 [Jolley et al., 2007b](#); [Ottesen Ellevset et al., 1998](#); [Tueckmantel et al., 2010](#)).  
732 A case study in the North Sea and Norwegian Continental Shelf plotted the  
733 permeability of fault rocks against the clay content of the host rocks for  
734 various fault rock types ([Fig.13](#)) ([Fisher and Knipe, 2001](#)). The case study  
735 suggests that for low throw faults with self-juxtaposition, the clean  
736 sandstones (clay content <15%) tend to form cataclasites that do not always  
737 represent effective fluid flow barriers; the impure sandstones (clay content  
738 15%-40%) experience significant porosity and permeability reduction; while  
739 the mudstones or shales form continuous clay smears with very low  
740 permeability that can be effective barriers for fluid flow across the fault  
741 zones. It also highlights that the permeability of the fault rocks is not only  
742 determined by the clay content of host rocks, but also related to their burial  
743 history ([Fig.13](#)). Different burial history implies that fault rocks have  
744 experienced different stress and temperature during fault deformation, which  
745 results in variable range of permeability of fault rocks. Therefore, the  
746 petrophysical assessment of fault rocks becomes an effective method to  
747 provide reliable poroperm results for the evaluation of fault sealing capacity.

748 Fig.13 Summary of the fault rock permeability from the North Sea and  
749 Norwegian Continental Shelf ([modified from Fisher and Knipe, 2001](#)).

750 The permeability of various fault rocks is plotted against the clay  
751 content of the host rocks. The chart also describes the control of the  
752 burial depth at the time of faulting and maximum post-deformation  
753 burial depth on the fault rock permeability.

## 754 **6.5. Production simulation modelling**

755 Production simulation modelling is an effective tool to predict the petroleum  
756 migration and accumulation characteristics in petroleum industry in the last  
757 decades. The accurate input of geologic data into the simulation model,  
758 particularly the data of fault zone architecture and fault rock properties, is  
759 vital to increase the confidence in the reliability of its predictive capability.  
760 Based on a series of case studies ([Fisher and Jolley, 2007](#); [Harris et al.,](#)  
761 [2007](#); [Jolley et al., 2007b](#); [Zijlstra et al., 2007](#)), [Fisher and Jolley \(2007\)](#)  
762 proposed several advices for those who would like to incorporate the effects  
763 of fault architecture on fluid flow in a production simulation model.

764 i) A geometrically accurate structural interpretation should not get compromised  
765 during transfer and incorporation into the production simulation model,  
766 particularly the fault zone geometry and fault compartmentalization.

767 ii) The transmissibility multipliers should be calculated based on realistic fluid  
768 flow properties of the fault rocks obtained within the field.

769 iii) Apart from single-phase permeability of the fault rocks, it is also of  
770 importance to consider the capillary pressure and relative permeability in some  
771 situation, particularly for high net: gross reservoirs with cataclastic fault rocks  
772 developed within the fault zone ([Al-Busafi et al., 2005](#); [Manzocchi et al., 2002](#)).

773 iv) As the interpretation of the data is often non-unique, caution must be given  
774 when concluding what the data actually reveal about fault-related fluid flow, in  
775 order to decrease the uncertainties being introduced into the production-related  
776 fault seal analysis.

777 The concept of 'fault facies' has also been proposed to define any features  
778 deriving its present properties from tectonic deformation, which can improve

779 the understanding the impact of fault zone architecture on hydrocarbon  
780 sealing behaviour (Tveranger et al., 2004; Tveranger et al., 2005). Originally,  
781 the concept of 'facies' is normally used to describe sedimentary rocks or  
782 metamorphic rocks. The introduction of fault facies allows the natural  
783 extension of the facies concept into the realm of both fault zone architecture  
784 and its fault rock properties (Braathen et al., 2009). As fault facies are  
785 associated to the fault geometry, internal structure, petrophysical properties  
786 and fault spatial distribution, it provides a novel approach to incorporate fault  
787 zone architecture and its impact on fluid flow properties into a three-  
788 dimensional production simulation model (Braathen et al., 2009; Fachri et al.,  
789 2013b; Fachri et al., 2011; Manzocchi et al., 2010).

## 790 **7. Factors affecting petrophysical properties of fault rocks**

791 The petrophysical properties of fault rocks are mainly determined by the  
792 clay/phyllsilicate content, the level of cataclasis and the amount of  
793 cementation (Fig.9) (Fisher and Knipe, 2001). However, in some natural  
794 oil/gas fields, the fault rocks, generated from sandstones with identical  
795 clay/phyllsilicate contents, can have different porosity and permeability  
796 characteristics (e.g. Fisher et al., 2003; Fisher and Knipe, 2001; Fossen et  
797 al., 2007). Based on a case study on the cataclastic faults from the  
798 Rotliegendes of the Southern North Sea, this can be attributed to the burial  
799 history that leads to interaction between the temperature history and the  
800 stress history (Fig.14), which can alter the petrophysical properties of fault  
801 rocks within the fault zones (Fisher and Knipe, 2001). For example, faults  
802 within the Rotliegendes formed at deeper depths than that in the Middle  
803 Jurassic reservoirs and therefore are closer to the temperature at which

804 quartz precipitates rapidly (Fig.14). Apart from temperature and stress  
805 history, geological time is a third factor influencing the permeability evolution  
806 of a fault zone, which means a same fault zone can present different sealing  
807 properties through geological time ([Indrevær et al., 2014](#)).

808 Fig.14 Data of cataclastic faults from the Rotliegendes of the Southern North  
809 Sea. The plots show (a) permeability against their maximum burial  
810 depth and (b) permeability contrast against their maximum burial depth  
811 ([Fisher and Knipe, 2001](#)).

## 812 **7.1. Temperature history**

813 It has been commonly accepted that the temperature history of fault rocks  
814 has a significant effect on the rate of meso-diagenesis, e.g., quartz  
815 cementation and pressure solution ([Walderhaug, 1996](#)). The rate usually  
816 increases as a function of temperature ([Fisher et al., 2003](#); [Fisher and Knipe,](#)  
817 [2001](#); [Fisher et al., 2009](#)), e.g., the quartz cementation and pressure solution  
818 occurs at rapid rate when the temperature exceeds ~90°C.

## 819 **7.2. Stress History**

820 Many studies tried to identify the effects of confining pressure on the  
821 deformation behaviour of faults/fault zones in sandstones. These studies  
822 suggest that: the sandstones at low confining pressures are likely to  
823 experience brittle faulting (failure occurs along single slip planes), while the  
824 sandstones at high confining pressures prefer more distributed ductile  
825 deformation without the generation of discrete slip planes (e.g. [Handin et al.,](#)  
826 [1963](#); [Scott and Nielsen, 1991](#)). The experimental studies indicate that the  
827 grain size and the permeability of faults/fault zones decrease with increasing

828 confining pressure and temperature (e.g. Crawford, 1998; Engelder, 1974;  
829 Fisher and Knipe, 2001; Zhu and Wong, 1997).

830 Therefore, as well as the clay/phyllsilicate content of host rocks, the effects  
831 of temperature history and stress history need to be taken into account when  
832 evaluating the fault sealing properties (Fisher et al., 2003; Fisher and Knipe,  
833 2001; Fossen et al., 2007; Jolley et al., 2007b). The schematic cartoons in  
834 Fig.15 demonstrate the potential effects of burial depth (increasing effective  
835 stress and temperature) on micro-structural deformation mechanisms (Jolley  
836 et al., 2007b). Firstly, the different fault seal processes do not always occur  
837 independently, and it is common to observe multiple fault seal processes in  
838 a same fault zone. Secondly, the occurrence of combinations of fault seal  
839 processes is determined by both the clay/phyllsilicate content and the burial  
840 depth, as these two factors control the clay/phyllsilicate content of the  
841 generated fault rocks and its deformation environment (stress &  
842 temperature).

843 Fig.15 Schematic cartoons of micro-structural deformation mechanisms with  
844 various fault rocks generated in different geological settings, e.g., clay  
845 content of the host rocks and burial depth (reflecting increasing  
846 effective stress and temperature) (modified from Jolley et al., 2007b).

### 847 **7.3. Cyclic evolution of permeability through geological time**

848 As a same fault zone can present different hydrocarbon sealing behaviour  
849 through geological time, it is of importance to understand the control of  
850 geological time on the permeability evolution of a fault zone (both cross and  
851 along a fault zone). Many studies, particularly on production simulation  
852 modelling, have investigated the role of geological time on fault zone

853 permeability evolution (Fisher and Knipe, 2001; Indrevær et al., 2014; Jolley  
854 et al., 2007b; Knipe et al., 1997; Manzocchi et al., 2010; Manzocchi et al.,  
855 2002). Indrevær et. al. (2014) proposed a model to demonstrate the cyclic  
856 permeability evolution of fault zones through geological time (Fig.16),  
857 describing faults as (i) conduits, (ii) barriers or (iii) conduits and barriers  
858 under different circumstances. At stage (a), the fault zone acts as fluid  
859 conduits as the porosity and permeability are increased by fracturing and  
860 cataclasis during faulting deformation. At stage (b), after the faulting  
861 deformation, the fault core zone acts as barriers whereas the damage zone  
862 acts as conduits for fluid flow, as the following precipitation of minerals and  
863 grain growth within the fault core zone inhibit the fluid flow. At stage (c), the  
864 entire fault zone is sealed by further grain growth and precipitation  
865 processes through time, and therefore acts as barriers for fluid flow, both  
866 along and across fault zone. At stage (d), a new permeability evolution cycle  
867 of the fault zone is restarted when the fault zone is reactivated in a later  
868 faulting deformation. Although this schematic permeability evolution model  
869 oversimplified many details associated with fault zone architecture and fault  
870 sealing properties, it reveals a basic cyclic changes of leakage and sealing  
871 across or along a fault zone through geological time.

872 Fig.16 Schematic illustration of a model showing the cyclic permeability  
873 evolution of fault zones through geological time (modified from  
874 [Indrevær et al., 2014](#)). (a) With faulting deformation, movement along a  
875 fault causes fracturing and cataclasis within the core zone and  
876 increases permeability. The core zone thereby acts as a fluid conduit.  
877 (b) Precipitation of minerals and grain growth within the core zone  
878 decreases permeability within the core zone and forces fluid flow into  
879 the damage zone. (c) Further grain growth and precipitation processes  
880 through time decrease porosity and permeability to gradually seal the  
881 entire fault zone. (d) Fault reactivation will initiate a new fluid flow  
882 evolution cycle.

## 883 **8. Limitations and future of fault seal analysis**

884 Fault seal analysis has been evolved since the concept of 'sealing' and 'non-  
885 sealing' was proposed by Smith in 1966 ([Smith, 1966](#)). In the past 50 years,  
886 by understanding the fault zone architecture, fault seal types, fault seal  
887 processes and generated fault rocks, geologists have proposed a bunch of  
888 models and methods to evaluate the hydrocarbon sealing behaviour of a  
889 fault zone. The initial application of Allan map ([Allan, 1989](#)) and triangle  
890 juxtaposition diagram ([Knipe, 1997](#)) makes it possible to investigate the  
891 effects of stratigraphic juxtaposition on the fluid flow properties of a fault  
892 zone. The later utilization of clay smear indices allows the quantitative  
893 evaluation of fault sealing capacity ([Bouvier et al., 1989](#); [Fulljames et al.,](#)  
894 [1997](#); [Lindsay et al., 1993](#); [Yielding et al., 1997](#)). The recent employment of  
895 SEM photography and petrophysical assessment enables the investigation  
896 of deformation mechanisms of fault rocks and their effects on grain size

897 reduction, porosity collapse and permeability decrease (e.g., Fisher et al.,  
898 2003; Fisher and Knipe, 1998; Fisher and Knipe, 2001; Fisher et al., 2009;  
899 Ottesen Ellevset et al., 1998). These methods have significantly boosted the  
900 fault seal related analysis in the past decades; however, there is still great  
901 potential for further progress in fault seal related research. The apparent  
902 limitations of the present-day models/methods have significantly constrained  
903 the effectiveness of fault seal analysis, such as:

904 a). Each individual model/method in present-day mostly focuses on a  
905 certain scale, which inhibits the 'extrapolation' of the results to a  
906 larger or smaller scale. A scale-dependent model/method may  
907 overlook the characteristics at its own scale while neglect that at other  
908 scales.

909 b). Further investigation and case studies are still necessary, as the  
910 present models/methods have not been sufficiently validated by  
911 physical simulation. The stratigraphic/mechanical heterogeneity  
912 contributes to high degree of fault zone complexity; therefore, the  
913 physical simulation is of great importance to validate the effectiveness  
914 of fault seal evaluation using present models/methods.

915 c). The present methods of fault seal analysis are mostly used to  
916 study the fault zone architecture and fault sealing properties in  
917 extensional regimes. Many case studies have realized that  
918 faults/fractures can play important control on the hydrocarbon  
919 migration in contractional regimes, e.g., the study in Kentucky, USA  
920 (Lewis et al., 2002), the New Guinea Fold Belt (Hill et al., 2004), the  
921 North West Borneo (Ingram et al., 2004), the Qaidam basin (Pang et

922 al., 2004), etc. However, the detailed thrust fault architecture  
923 (particularly the meso- to micro-scale deformation features) and its  
924 effect on the fault sealing behaviour have not been well studied in  
925 contractional systems.

926 d). The concept of 'fault facies', associated to the fault geometry,  
927 internal structure, petrophysical properties and fault spatial  
928 distribution, is apparently an effective approach for incorporating both  
929 fault zone architecture and its impact on fluid flow properties into a  
930 three-dimensional production simulation model. However, further  
931 studies on fault facies are necessary to find how to apply this concept  
932 in different geological settings.

933 Considering the limitations of present fault seal analysis methods, there are  
934 a number of general paths to improve the fault seal analysis, for instance:

935 a). Multi-approach/scale investigation should be the direction for  
936 further fault seal analysis. The results from an individual  
937 model/method, however good, is of much less value if it was highly  
938 scale-dependent. The multi-approach/scale fault seal analysis can  
939 avoid the scale-limitation of the results.

940 b). Further fluid flow physical simulation of fault zones could be  
941 employed to validate the fault seal analysis using the existing  
942 models/methods. Fluid flow physical simulation can be an effective  
943 'ground-truthing' tool to discriminate these models/methods as to their  
944 accuracy of prediction in particular natural fault zones. A  
945 model/method can be an effective model/method only if it was  
946 sufficiently tested by 'ground-truthing' tools.

947 c). Fault seal analysis in contractional systems should be taken into  
948 account. It is of great value to understand the differences of fault  
949 sealing properties between contractional and extensional regimes,  
950 particularly in the aspects of fault architecture, fault seal processes  
951 and their effects on fluid flow properties.

952 d).Fault facies should be integrated into the production simulation  
953 model to predict the impact of fault architecture on hydrocarbon  
954 sealing behaviour within a fault zone.

## 955 **9. Conclusions**

956 Fault sealing properties is one of the most important aspects of fault zone  
957 associated research. By understanding the fault zone architecture, fault seal  
958 types, fault seal processes and generated fault rocks, geologists have  
959 proposed different models and methods to evaluate the hydrocarbon sealing  
960 behaviour of a fault zone in the past decades. The proposal of these  
961 models/methods has significantly promoted the application of fault seal  
962 analysis to natural fault zones.

963 The present models/methods have clearly enhanced the understanding of  
964 fault zone sealing behaviour; however, further fault seal analysis should  
965 consider multi-approach/scale and physical simulation, in both extensional  
966 and contractional regimes.

## 967 **Acknowledgements**

968 It is impossible to finish this manuscript without the discussion and  
969 suggestions from many colleagues over recent years. We would like to thank  
970 Dr J. Geoff Lloyd, Dr Jonathan Imber, Dr Anren Li, Dr Henry Lickorish, and

971 Prof Xin Wang for the good communications contributing to this review  
972 article. The constructive comments and suggestions from both the editor (Dr.  
973 Carlo Doglioni) and two reviewers (Dr. Fabrizio Agosta and Dr. Kim Senger)  
974 are of great use to this work and greatly appreciated. This work has been  
975 collaboratively supported by the Fundamental Research Funds for the  
976 Central Universities (15CX02004A), Shandong Provincial Natural Science  
977 Foundation China (2014BSE28008, ZR2012DM011) and National Natural  
978 Science Foundation of China (41272142).

979 **References**

- 980 Agosta, F., Ruano, P., Rustichelli, A., Tondi, E., Galindo-Zaldívar, J. and  
981 Sanz de Galdeano, C., 2012. Inner structure and deformation  
982 mechanisms of normal faults in conglomerates and carbonate  
983 grainstones (Granada Basin, Betic Cordillera, Spain): Inferences on  
984 fault permeability. *Journal of Structural Geology*, 45(0): 4-20.
- 985 Al-Busafi, B., Fisher, Q.J. and Harris, S.D., 2005. The importance of  
986 incorporating the multi-phase flow properties of fault rocks into  
987 production simulation models. *Marine and Petroleum Geology*, 22(3):  
988 365-374.
- 989 Allan, U.S., 1989. Model for Hydrocarbon Migration and Entrapment within  
990 Faulted Structures. *American Association of Petroleum Geologists  
991 Bulletin*, 73(7): 803-811.
- 992 Antonellini, M. and Aydin, A., 1994. Effect of Faulting on Fluid-Flow in  
993 Porous Sandstones - Petrophysical Properties. *American Association  
994 of Petroleum Geologists Bulletin*, 78(3): 355-377.
- 995 Antonellini, M. and Aydin, A., 1995. Effect of Faulting on Fluid-Flow  
996 Geometry and Spatial-Distribution. *American Association of  
997 Petroleum Geologists Bulletin*, 79(5): 642-671.
- 998 Antonellini, M.A., Aydin, A. and Pollard, D.D., 1994. Microstructure of  
999 deformation bands in porous sandstones at Arches National Park,  
1000 Utah. *Journal of Structural Geology*, 16(7): 941-959.
- 1001 Aydin, A. and Eyal, Y., 2002. Anatomy of a normal fault with shale smear:  
1002 Implications for fault seal. *Aapg Bulletin-American Association of  
1003 Petroleum Geologists*, 86(8): 1367-1381.
- 1004 Balsamo, F., Storti, F., Salvini, F., Silva, A.T. and Lima, C.C., 2010.  
1005 Structural and petrophysical evolution of extensional fault zones in  
1006 low-porosity, poorly lithified sandstones of the Barreiras Formation,  
1007 NE Brazil. *Journal of Structural Geology*, 32(11): 1806-1826.
- 1008 Bense, V., Van den Berg, E. and Van Balen, R., 2003. Deformation  
1009 mechanisms and hydraulic properties of fault zones in unconsolidated  
1010 sediments; the Roer Valley Rift System, The Netherlands.  
1011 *Hydrogeology Journal*, 11(3): 319-332.
- 1012 Billi, A., Salvini, F. and Storti, F., 2003. The damage zone-fault core  
1013 transition in carbonate rocks: implications for fault growth, structure  
1014 and permeability. *Journal of Structural Geology*, 25(11): 1779-1794.
- 1015 Bjorkum, P.A., 1996. How important is pressure in causing dissolution of  
1016 quartz in sandstones? *Journal of Sedimentary Research*, 66(1): 147-  
1017 154.
- 1018 Blenkinsop, T.G., 1991. Cataclasis and processes of particle size reduction.  
1019 *Pure and Applied Geophysics*, 136(1): 59-86.
- 1020 Borg, I., Friedman, M., Handin, J. and Higgs, D.V., 1960. Chapter 6:  
1021 Experimental Deformation of St. Peter Sand: A Study of Cataclastic  
1022 Flow. *Geological Society of America Memoirs*, 79: 133-192.
- 1023 Bouvier, J.D., Kaarssijpesteijn, C.H., Kluesner, D.F., Onyejekwe, C.C. and  
1024 Vanderpal, R.C., 1989. Three-Dimensional Seismic Interpretation and  
1025 Fault Sealing Investigations, Nun River Field, Nigeria. *American  
1026 Association of Petroleum Geologists Bulletin*, 73(11): 1397-1414.

- 1027 Braathen, A., Tveranger, J., Fossen, H., Skar, T., Cardozo, N., Semshaug,  
1028 S., Bastesen, E. and Sverdrup, E., 2009. Fault facies and its  
1029 application to sandstone reservoirs. *AAPG bulletin*, 93(7): 891-917.
- 1030 Brogi, A. and Novellino, R., 2015. Low Angle Normal Fault (LANF)-zone  
1031 architecture and permeability features in bedded carbonate from inner  
1032 Northern Apennines (Rapolano Terme, Central Italy). *Tectonophysics*,  
1033 638(0): 126-146.
- 1034 Caine, J.S., Evans, J.P. and Forster, C.B., 1996. Fault zone architecture and  
1035 permeability structure. *Geology*, 24(11): 1025-1028.
- 1036 Cecil, C.B. and Heald, M.T., 1971. Experimental investigation of the effects  
1037 of grain coatings on quartz growth. *Journal of Sedimentary Petrology*,  
1038 41: 582-584.
- 1039 Cervený, K., Davies, R., Dudley, G., Fox, R., Kaufman, P., Knipe, R.J. and  
1040 Krantz, B., 2004. Reducing Uncertainty with Fault-Seal Analysis.  
1041 *Oilfield Review*, 16(4): 38-51.
- 1042 Childs, C., Manzocchi, T., Walsh, J.J., Bonson, C.G., Nicol, A. and Schöpfer,  
1043 M.P.J., 2009. A geometric model of fault zone and fault rock thickness  
1044 variations. *Journal of Structural Geology*, 31(2): 117-127.
- 1045 Childs, C., Nicol, A., Walsh, J.J. and Watterson, J., 1996a. Growth of  
1046 vertically segmented normal faults. *Journal of Structural Geology*,  
1047 18(12): 1389-1397.
- 1048 Childs, C., Watterson, J. and Walsh, J.J., 1996b. A model for the structure  
1049 and development of fault zones. *Journal of the Geological Society*,  
1050 153(3): 337-340.
- 1051 Choi, J.H., Yang, S.J., Han, S.R. and Kim, Y.S., 2015. Fault zone evolution  
1052 during Cenozoic tectonic inversion in SE Korea. *Journal of Asian  
1053 Earth Sciences*, 98: 167–177.
- 1054 Ciftci, N.B., Giger, S.B. and Clennell, M.B., 2013. Three-dimensional  
1055 structure of experimentally produced clay smears: Implications for  
1056 fault seal analysis. *American Association of Petroleum Geologists  
1057 Bulletin*, 97(5): 733-757.
- 1058 Clarke, S.M., Burley, S.D. and Williams, G.D., 2005. A three-dimensional  
1059 approach to fault seal analysis: fault-block juxtaposition & argillaceous  
1060 smear modelling. *Basin Research*, 17(2): 269-288.
- 1061 Collettini, C., Carpenter, B.M., Viti, C., Cruciani, F., Mollo, S., Tesei, T.,  
1062 Trippetta, F., Valoroso, L. and Chiaraluce, L., 2014. Fault structure  
1063 and slip localization in carbonate-bearing normal faults: An example  
1064 from the Northern Apennines of Italy. *Journal of Structural Geology*,  
1065 67, Part A(0): 154-166.
- 1066 Cowie, P.A., Knipe, R.J. and Main, I.G., 1996. Introduction to the Special  
1067 Issue: Scaling Laws for fault and fracture populations - analyses and  
1068 applications. *Journal of Structural Geology*, 18(2-3): v-xi.
- 1069 Cowie, P.A. and Scholz, C.H., 1992. Displacement-length scaling  
1070 relationship for faults: data synthesis and discussion. *Journal of  
1071 Structural Geology*, 14(10): 1149-1156.
- 1072 Cowie, P.A., Vanneste, C. and Sornette, D., 1993. Statistical physics model  
1073 for the spatiotemporal evolution of faults. *Journal of Geophysical  
1074 Research*, 98(B12): 21809-21821.
- 1075 Crawford, B.R., 1998. Experimental fault sealing: shear band permeability  
1076 dependency on cataclastic fault gouge characteristics. *Geological  
1077 Society, London, Special Publications*, 127(1): 27-47.

- 1078 Davatzes, N. and Aydin, A., 2005. Distribution and nature of fault  
1079 architecture in a layered sandstone and shale sequence: An example  
1080 from the Moab fault, Utah. in R. Sorkhabi and Y. Tsuji, eds., Faults,  
1081 fluid flow, and petroleum traps: American Association of Petroleum  
1082 Geologists Memoir, 85: 153-180.
- 1083 Dewers, T. and Ortoleva, P., 1991. Influences of clay minerals on sandstone  
1084 cementation and pressure solution. *Geology*, 19(10): 1045-1048.
- 1085 Dewers, T. and Ortoleva, P.J., 1990. Interaction of reaction, mass transport,  
1086 and rock deformation during diagenesis: mathematical modelling of  
1087 intergranular pressure solution, stylolites, and differential  
1088 compaction/cementation. in I. D. Meshri and P. J. Ortoleva, eds.,  
1089 Prediction of Reservoir Quality through Chemical Modelling: American  
1090 Association of Petroleum Geologists Memoir, 49: 147-160.
- 1091 Egholm, D.L., Clausen, O.R., Sandiford, M., Kristensen, M.B. and Korstgård,  
1092 J.A., 2008. The mechanics of clay smearing along faults. *Geology*,  
1093 36(10): 787-790.
- 1094 Eisenstadt, G. and De Paor, D.G., 1987. Alternative model of thrust-fault  
1095 propagation. *Geology*, 15(7): 630-633.
- 1096 Engelder, J.T., 1974. Cataclasis and the Generation of Fault Gouge.  
1097 *Geological Society of America Bulletin*, 85(10): 1515-1522.
- 1098 Fachri, M., Rotevatn, A. and Tveranger, J., 2013a. Fluid flow in relay zones  
1099 revisited: Towards an improved representation of small-scale  
1100 structural heterogeneities in flow models. *Marine and Petroleum  
1101 Geology*, 46(0): 144-164.
- 1102 Fachri, M., Tveranger, J., Braathen, A. and Schueller, S., 2013b. Sensitivity  
1103 of fluid flow to deformation-band damage zone heterogeneities: A  
1104 study using fault facies and truncated Gaussian simulation. *Journal of  
1105 Structural Geology*, 52: 60-79.
- 1106 Fachri, M., Tveranger, J., Cardozo, N. and Pettersen, O., 2011. The impact  
1107 of fault envelope structure on fluid flow: A screening study using fault  
1108 facies. *AAPG bulletin*, 95(4): 619-648.
- 1109 Faulkner, D.R., Jackson, C.A.L., Lunn, R.J., Schlische, R.W., Shipton, Z.K.,  
1110 Wibberley, C.A.J. and Withjack, M.O., 2010. A review of recent  
1111 developments concerning the structure, mechanics and fluid flow  
1112 properties of fault zones. *Journal of Structural Geology*, 32(11): 1557-  
1113 1575.
- 1114 Faulkner, D.R., Lewis, A.C. and Rutter, E.H., 2003. On the internal structure  
1115 and mechanics of large strike-slip fault zones: field observations of  
1116 the Carboneras fault in southeastern Spain. *Tectonophysics*, 367(3):  
1117 235–251.
- 1118 Fisher, Q.J., Casey, M., Harris, S.D. and Knipe, R.J., 2003. Fluid-flow  
1119 properties of faults in sandstone: The importance of temperature  
1120 history. *Geology*, 31(11): 965-968.
- 1121 Fisher, Q.J. and Jolley, S.J., 2007. Treatment of faults in production  
1122 simulation models. Geological Society, London, Special Publications,  
1123 292: 219-233.
- 1124 Fisher, Q.J. and Knipe, R.J., 1998. Fault sealing processes in siliciclastic  
1125 sediments. Geological Society, London, Special Publications, 147:  
1126 117-134.
- 1127 Fisher, Q.J. and Knipe, R.J., 2001. The permeability of faults within  
1128 siliciclastic petroleum reservoirs of the North Sea and Norwegian

- 1129 Continental Shelf. *Marine and Petroleum Geology*, 18(10): 1063-  
1130 1081.
- 1131 Fisher, Q.J., Knipe, R.J. and Worden, R.H., 2009. Microstructures of  
1132 Deformed and Non-Deformed Sandstones from the North Sea:  
1133 Implications for the Origins of Quartz Cement in Sandstones. in R. H.  
1134 Worden and S. Morad, eds., *Quartz Cementation in Sandstones*,  
1135 Blackwell Publishing Ltd., Oxford, UK, 14: 129-146.
- 1136 Fondriest, M., Smith, S.A.F., Toro, G.D., Zampieri, D. and Mitterpergher, S.,  
1137 2012. Fault zone structure and seismic slip localization in dolostones,  
1138 an example from the Southern Alps, Italy. *Journal of Structural*  
1139 *Geology*, 45: 52–67.
- 1140 Fossen, H. and Bale, A., 2007. Deformation bands and their influence on  
1141 fluid flow. *Aapg Bulletin*, 91(12): 1685-1700.
- 1142 Fossen, H., Schultz, R.A., Shipton, Z.K. and Mair, K., 2007. Deformation  
1143 bands in sandstone: a review. *Journal of the Geological Society*,  
1144 164(4): 755-769.
- 1145 Fossen, H., Schultz, R.A. and Torabi, A., 2011. Conditions and implications  
1146 for compaction band formation in the Navajo Sandstone, Utah.  
1147 *Journal of Structural Geology*, 33(10): 1477-1490.
- 1148 Fulljames, J.R., Zijerveld, L.J.J. and Franssen, R.C.M.W., 1997. Fault seal  
1149 processes: systematic analysis of fault seals over geological and  
1150 production time scales. In: P. Møller-Pedersen and A.G. Koestler  
1151 (Editors), *Norwegian Petroleum Society Special Publications*, pp. 51-  
1152 59.
- 1153 Gibson, R.G., 1994. Fault-Zone Seals in Siliciclastic Strata of the Columbus  
1154 Basin, Offshore Trinidad. *American Association of Petroleum*  
1155 *Geologists Bulletin*, 78(9): 1372-1385.
- 1156 Handin, J., Hager Jr, R.V., Friedman, M. and Feather, J.N., 1963.  
1157 Experimental deformation of sedimentary rocks under confining  
1158 pressure: pore pressure tests. *American Association of Petroleum*  
1159 *Geologists Bulletin*, 47(5): 717-755.
- 1160 Harris, S.D., Vaszi, A.Z. and Knipe, R.J., 2007. Three-dimensional upscaling  
1161 of fault damage zones for reservoir simulation. *Geological Society*,  
1162 London, *Special Publications*, 292: 353-374.
- 1163 Heald, M.T., 1955. Stylolites in Sandstones. *The Journal of Geology*, 63(2):  
1164 101-114.
- 1165 Heynekamp, M.R., Goodwin, L.B., Mozley, P.S. and Haneberg, W.C., 1999.  
1166 Controls on fault-zone architecture in poorly lithified sediments, Rio  
1167 Grande Rift, New Mexico: Implications for fault-zone permeability and  
1168 fluid flow, *Faults and Subsurface Fluid Flow in the Shallow Crust*.  
1169 Washington, DC, AGU. *Geophys. Monogr. Ser.*, pp. 27-49.
- 1170 Hill, K.C., Keetley, J.T., Kendrick, R.D. and Sutriyono, E., 2004. Structure  
1171 and hydrocarbon potential of the New Guinea Fold Belt. in K. R.  
1172 McClay, eds., *Thrust tectonics and hydrocarbon systems: American*  
1173 *Association of Petroleum Geologists Memoir*, 82: 494-514.
- 1174 Indrevær, K., Stunitz, H. and Bergh, S.G., 2014. On Palaeozoic–Mesozoic  
1175 brittle normal faults along the SW Barents Sea margin: fault  
1176 processes and implications for basement permeability and margin  
1177 evolution. *Journal of the Geological Society*, 171(6): 831-846.
- 1178 Ingram, G.M., Chisholm, T.J., Grant, C.J., Hedlund, C.A., Stuart-Smith, P.  
1179 and Teasdale, J., 2004. Deepwater North West Borneo: hydrocarbon

1180 accumulation in an active fold and thrust belt. *Marine and Petroleum*  
1181 *Geology*, 21(7): 879-887.

1182 Jolley, S.J., Barr, D., Walsh, J.J. and Knipe, R.J., 2007a. Structurally  
1183 complex reservoirs: an introduction. Geological Society, London,  
1184 Special Publications, 292: 1-24.

1185 Jolley, S.J., Dijk, H., Lamens, J.H., Fisher, Q.J., Manzocchi, T., Eikmans, H.  
1186 and Huang, Y., 2007b. Faulting and fault sealing in production  
1187 simulation models: Brent Province, northern North Sea. *Petroleum*  
1188 *Geoscience*, 13(4): 321-340.

1189 Jones, R.M. and Hillis, R.R., 2003. An integrated, quantitative approach to  
1190 assessing fault-seal risk. *AAPG bulletin*, 87(3): 507-524.

1191 Knipe, R.J., 1989. Deformation Mechanisms - Recognition from Natural  
1192 Tectonites. *Journal of Structural Geology*, 11(1-2): 127-146.

1193 Knipe, R.J., 1992a. Faulting processes and fault seal. In: R.M. Larsen, H.  
1194 Brekke, B.T. Larsen and E. Talleraas (Editors), *Norwegian Petroleum*  
1195 *Society Special Publications*, pp. 325-342.

1196 Knipe, R.J., 1992b. Faulting processes, seal evolution, and reservoir  
1197 discontinuities: An integrated analysis of the ULA Field, Central  
1198 Graben, North Sea, Abstracts of the Petroleum Group meeting on  
1199 collaborative research programme in petroleum geoscience between  
1200 UK Higher Education Institutes and the Petroleum Industry,  
1201 Geological Society, London.

1202 Knipe, R.J., 1993a. The Influence of Fault Zone Processes and Diagenesis  
1203 on Fluid Flow. *Diagenesis and Basin Development*(36): 135-154.

1204 Knipe, R.J., 1993b. Micromechanisms of deformation and fluid flow  
1205 behaviour during faulting. The mechanical behavior of fluids in fault  
1206 zones: USGS Open-File Report: 94-228.

1207 Knipe, R.J., 1994. Fault zone geometry and behaviour: the importance of  
1208 damage zone evolution. Abstracts of Meetings Modern Developments  
1209 in Structural Interpretation, Geological Society, London.

1210 Knipe, R.J., 1997. Juxtaposition and seal diagrams to help analyze fault  
1211 seals in hydrocarbon reservoirs. *American Association of Petroleum*  
1212 *Geologists Bulletin*, 81(2): 187-195.

1213 Knipe, R.J., Fisher, R.J., Jones, G., Clennell, M.R., Farmer, A.B., Harrison,  
1214 a., Kidd, B., McAllister, E., R., P.J. and White, E.A., 1997. Fault seal  
1215 analysis: successful methodologies, application and future directions.  
1216 *Norwegian Petroleum Society Special Publications*, 7: 15-40.

1217 Knipe, R.J., Jones, G. and Fisher, Q.J., 1998. Faulting, fault sealing and fluid  
1218 flow in hydrocarbon reservoirs: an introduction. Geological Society,  
1219 London, Special Publications, 147(1): vii-xxi.

1220 Knott, S.D., 1993. Fault Seal Analysis in the North-Sea. *American*  
1221 *Association of Petroleum Geologists Bulletin*, 77(5): 778-792.

1222 Kolyukhin, D., Schueller, S., Espedal, M. and Fossen, H., 2010. Deformation  
1223 band populations in fault damage zone—impact on fluid flow.  
1224 *Computational Geosciences*, 14(2): 231-248.

1225 Korneva, I., Tondi, E., Agosta, F., Rustichelli, A., Spina, V., Bitonte, R. and  
1226 Di Cuia, R., 2014. Structural properties of fractured and faulted  
1227 Cretaceous platform carbonates, Murge Plateau (southern Italy).  
1228 *Marine and Petroleum Geology*, 57: 312-326.

1229 Lewis, G., Knipe, R.J. and Li, A., 2002. Fault seal analysis in unconsolidated  
1230 sediments: a field study from kentucky, USA. In: G.K. Andreas and H.

- 1231 Robert (Editors), Norwegian Petroleum Society Special Publications,  
1232 pp. 243-253.
- 1233 Lindsay, N.G., Murphy, F.C., Walsh, J.J. and Watterson, J., 1993. Outcrop  
1234 Studies of Shale Smears on Fault Surface, The Geological Modelling  
1235 of Hydrocarbon Reservoirs and Outcrop Analogues. Blackwell  
1236 Publishing Ltd., pp. 113-123.
- 1237 Loveless, S., Bense, V. and Turner, J., 2011. Fault architecture and  
1238 deformation processes within poorly lithified rift sediments, Central  
1239 Greece. *Journal of Structural Geology*, 33(11): 1554-1568.
- 1240 Manzocchi, T., Childs, C. and Walsh, J.J., 2010. Faults and fault properties  
1241 in hydrocarbon flow models. *Geofluids*, 10(1-2): 94-113.
- 1242 Manzocchi, T., Heath, A.E., Walsh, J.J. and Childs, C., 2002. The  
1243 representation of two phase fault-rock properties in flow simulation  
1244 models. *Petroleum Geoscience*, 8(2): 119-132.
- 1245 Manzocchi, T., Walsh, J.J., Nell, P. and Yielding, G., 1999. Fault  
1246 transmissibility multipliers for flow simulation models. *Petroleum  
1247 Geoscience*, 5(1): 53-63.
- 1248 McGrath, A.G. and Davison, I., 1995. Damage zone geometry around fault  
1249 tips. *Journal of Structural Geology*, 17(7): 1011-1024.
- 1250 Odling, N.E., Harris, S.D. and Knipe, R., 2004. Permeability scaling  
1251 properties of fault damage zones in siliclastic rocks. *Journal of  
1252 Structural Geology*, 26(9): 1727-1747.
- 1253 Oelkers, E.H., Bjorkum, P.A. and Murphy, W.M., 1996. A petrographic and  
1254 computational investigation of quartz cementation and porosity  
1255 reduction in North Sea sandstones. *American Journal of Science*,  
1256 296(4): 420-452.
- 1257 Ottesen Ellevset, S., Knipe, R.J., Svava Olsen, T., Fisher, Q.J. and Jones,  
1258 G., 1998. Fault controlled communication in the Sleipner Vest Field,  
1259 Norwegian Continental Shelf; detailed, quantitative input for reservoir  
1260 simulation and well planning. Geological Society, London, Special  
1261 Publications, 147(1): 283-297.
- 1262 Pang, X.Q., Li, Y.X. and Jiang, Z.X., 2004. Key geological controls on  
1263 migration and accumulation for hydrocarbons derived from mature  
1264 source rocks in Qaidam Basin. *Journal of Petroleum Science and  
1265 Engineering*, 41(1-3): 79-95.
- 1266 Peacock, D.C.P. and Sanderson, D.J., 1991. Displacements, segment  
1267 linkage and relay ramps in normal fault zones. *Journal of Structural  
1268 Geology*, 13(6): 721-733.
- 1269 Peacock, D.C.P. and Sanderson, D.J., 1992. Effects of layering and  
1270 anisotropy on fault geometry. *Journal of the Geological Society*,  
1271 149(5): 793-802.
- 1272 Peacock, D.C.P. and Sanderson, D.J., 1994. Geometry and development of  
1273 relay ramps in normal fault systems. *American Association of  
1274 Petroleum Geologists Bulletin*, 78(2): 147-165.
- 1275 Pei, Y.W., 2013. Thrust fault evolution and hydrocarbon sealing behaviour,  
1276 Qaidam basin, China. PhD Thesis, University of Leeds.
- 1277 Qu, D., Røe, P. and Tveranger, J., 2015. A method for generating volumetric  
1278 fault zone grids for pillar gridded reservoir models. *Computers &  
1279 Geosciences*, 81: 28-37.

- 1280 Rawling, G.C. and Goodwin, L.B., 2003. Cataclasis and particulate flow in  
1281 faulted, poorly lithified sediments. *Journal of Structural Geology*,  
1282 25(3): 317-331.
- 1283 Rawling, G.C. and Goodwin, L.B., 2006. Structural record of the mechanical  
1284 evolution of mixed zones in faulted poorly lithified sediments, Rio  
1285 Grande rift, New Mexico, USA. *Journal of Structural Geology*, 28(9):  
1286 1623-1639.
- 1287 Rawling, G.C., Goodwin, L.B. and Wilson, J.L., 2001. Internal architecture,  
1288 permeability structure, and hydrologic significance of contrasting fault-  
1289 zone types. *Geology*, 29(1): 43-46.
- 1290 Roche, V., Homberg, C. and Rocher, M., 2012. Architecture and growth of  
1291 normal fault zones in multilayer systems: A 3D field analysis in the  
1292 South-Eastern Basin, France. *Journal of Structural Geology*, 37(0):  
1293 19-35.
- 1294 Rotevatn, A. and Bastesen, E., 2014. Fault linkage and damage zone  
1295 architecture in tight carbonate rocks in the Suez Rift (Egypt):  
1296 implications for permeability structure along segmented normal faults.  
1297 *Geological Society, London, Special Publications*, 374(1): 79-95.
- 1298 Rotevatn, A., Fossen, H., Hesthammer, J., Aas, T.E. and Howell, J.A., 2007.  
1299 Are relay ramps conduits for fluid flow? Structural analysis of a relay  
1300 ramp in Arches National Park, Utah: in. *Geological Society of London*,  
1301 270(1).
- 1302 Rutter, E.H., 1983. Pressure solution in nature, theory and experiment.  
1303 *Journal of the Geological Society*, 140(5): 725-740.
- 1304 Schöpfer, M.P.J., Childs, C. and Walsh, J.J., 2006. Localisation of normal  
1305 faults in multilayer sequences. *Journal of Structural Geology*, 28(5):  
1306 816-833.
- 1307 Schowalter, T.T., 1979. Mechanics of secondary hydrocarbon migration and  
1308 entrapment. *American Association of Petroleum Geologists Bulletin*,  
1309 63(5): 723-760.
- 1310 Schultz, R.A. and Fossen, H., 2008. Terminology for structural  
1311 discontinuities. *Aapg Bulletin*, 92(7): 853-867.
- 1312 Scott, T.E. and Nielsen, K.C., 1991. The Effects of Porosity on the Brittle-  
1313 Ductile Transition in Sandstones. *Journal of Geophysical Research*,  
1314 96(B1): 405-414.
- 1315 Smith, D.A., 1966. Theoretical considerations of sealing and non-sealing  
1316 faults. *American Association of Petroleum Geologists Bulletin*, 50(2):  
1317 363-374.
- 1318 Smith, D.A., 1980. Sealing and nonsealing faults in Louisiana Gulf Coast salt  
1319 basin. *American Association of Petroleum Geologists Bulletin*, 64(2):  
1320 145-172.
- 1321 Spiers, C.J. and Schutjens, P.M.T.M., 1990. Densification of crystalline  
1322 aggregates by fluid-phase diffusional creep, *Deformation Processes*  
1323 *in Minerals, Ceramics and Rocks. The Mineralogical Society Series.*  
1324 *Springer Netherlands*, pp. 334-353.
- 1325 Tada, R. and Siever, R., 1989. Pressure Solution during Diagenesis. *Annual*  
1326 *Review of Earth and Planetary Sciences*, 17: 89-118.
- 1327 Torabi, A. and Berg, S.S., 2011. Scaling of fault attributes: A review. *Marine*  
1328 *and Petroleum Geology*, 28(8): 1444-1460.
- 1329 Tueckmantel, C., Fisher, Q.J., Knipe, R.J., Lickorish, H. and Khalil, S.M.,  
1330 2010. Fault seal prediction of seismic-scale normal faults in porous

1331 sandstone: A case study from the eastern Gulf of Suez rift, Egypt.  
1332 Marine and Petroleum Geology, 27(2): 334-350.

1333 Tveranger, J., Skar, T. and Braathen, A., 2004. Incorporation of fault zones  
1334 as volumes in reservoir models. Bolletino di Geofisica Teoretica et  
1335 Applicata, 45: 316-318.

1336 Tveranger, J., Skauge, A., Braathen, A. and Skar, T., 2005. Centre for  
1337 integrated petroleum research: Research activities with emphasis on  
1338 fluid flow in fault zones. Norsk Geologisk Tidsskrift, 85(1-2): 63-71.

1339 Walderhaug, O., 1996. Kinetic modeling of quartz cementation and porosity  
1340 loss in deeply buried sandstone reservoirs. American Association of  
1341 Petroleum Geologists Bulletin, 80(5): 731-745.

1342 Walsh, J.J., Bailey, W.R., Childs, C., Nicol, A. and Bonson, C.G., 2003.  
1343 Formation of segmented normal faults: a 3-D perspective. Journal of  
1344 Structural Geology, 25(8): 1251-1262.

1345 Walsh, J.J., Watterson, J., Bailey, W.R. and Childs, C., 1999. Fault relays,  
1346 bends and branch-lines. Journal of Structural Geology, 21(8-9):  
1347 1019-1026.

1348 Walsh, J.J., Watterson, J., Heath, A.E. and Childs, C., 1998. Representation  
1349 and scaling of faults in fluid flow models. Petroleum Geoscience, 4(3):  
1350 241-251.

1351 Watts, N.L., 1987. Theoretical aspects of cap-rock and fault seals for single-  
1352 and two-phase hydrocarbon columns. Marine and Petroleum  
1353 Geology, 4(4): 274-307.

1354 Welch, M.J., Davies, R.K., Knipe, R.J. and Tueckmantel, C., 2009a. A  
1355 dynamic model for fault nucleation and propagation in a mechanically  
1356 layered section. Tectonophysics, 474(3-4): 473-492.

1357 Welch, M.J., Knipe, R.J., Souque, C. and Davies, R.K., 2009b. A Quadshear  
1358 kinematic model for folding and clay smear development in fault  
1359 zones. Tectonophysics, 471(3-4): 186-202.

1360 Welch, M.J., Souque, C., Davies, R.K. and Knipe, R.J., 2015. Using  
1361 mechanical models to investigate the controls on fracture geometry  
1362 and distribution in chalk. Geological Society, London, Special  
1363 Publications, 406(1): 281-309.

1364 Yielding, G., Freeman, B. and Needham, D.T., 1997. Quantitative fault seal  
1365 prediction. American Association of Petroleum Geologists Bulletin,  
1366 81(6): 897-917.

1367 Yielding, G., Needham, T. and Jones, H., 1996. Sampling of fault  
1368 populations using sub-surface data: a review. Journal of Structural  
1369 Geology, 18(2): 135-146.

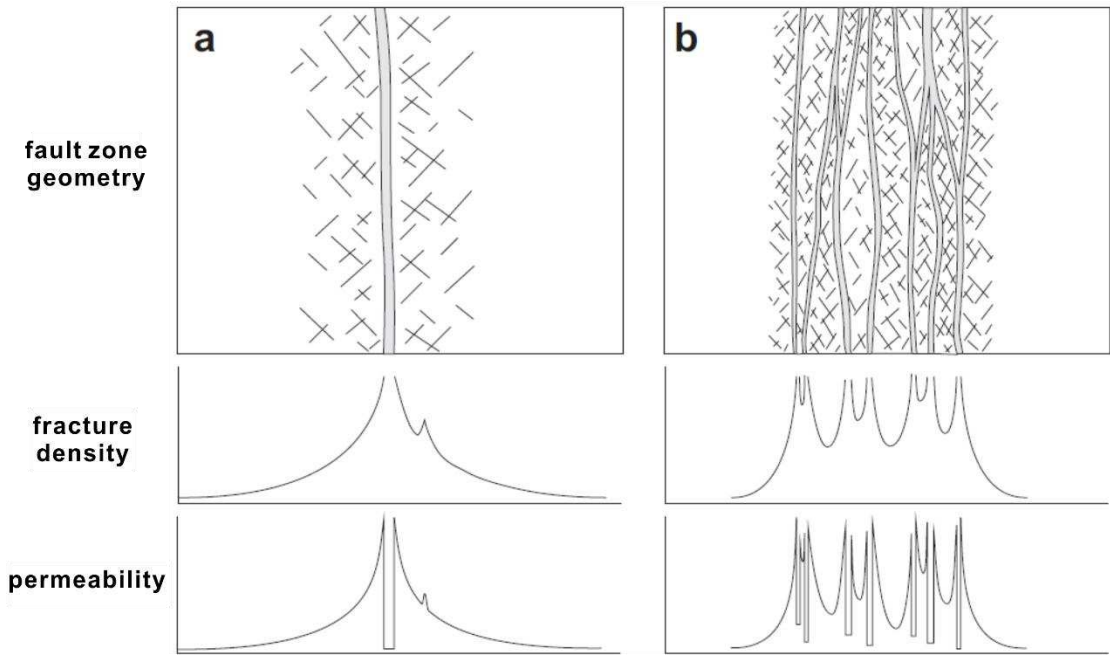
1370 Zhu, W.L. and Wong, T.F., 1997. The transition from brittle faulting to  
1371 cataclastic flow: Permeability evolution. Journal of Geophysical  
1372 Research, 102(B2): 3027-3041.

1373 Zijlstra, E.B., Reemst, P.H.M. and Fisher, Q.J., 2007. Incorporation of fault  
1374 properties into production simulation models of Permian reservoirs  
1375 from the southern North Sea. Geological Society, London, Special  
1376 Publications, 292: 295-308.

1377

1378

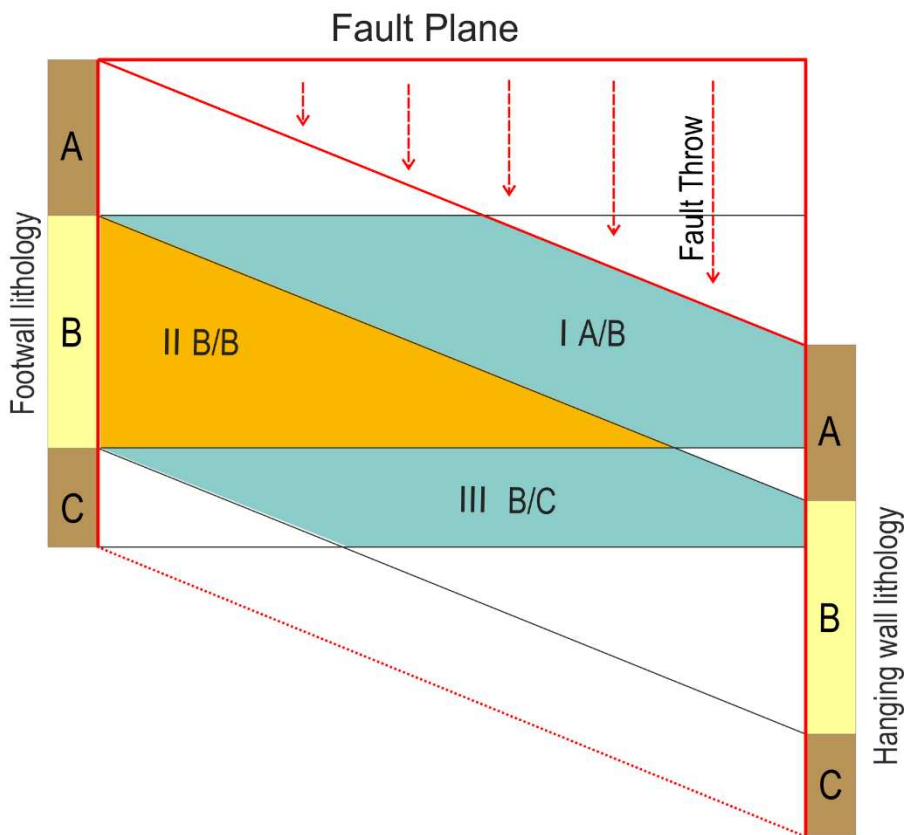
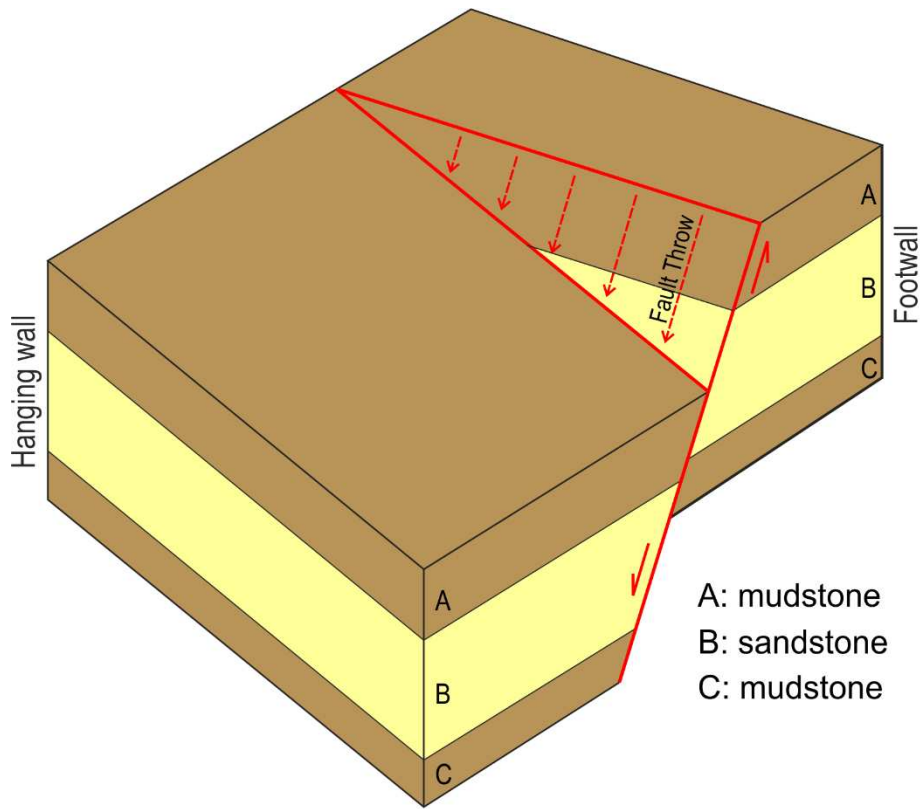
1379 **Figure 1**



1380

1381

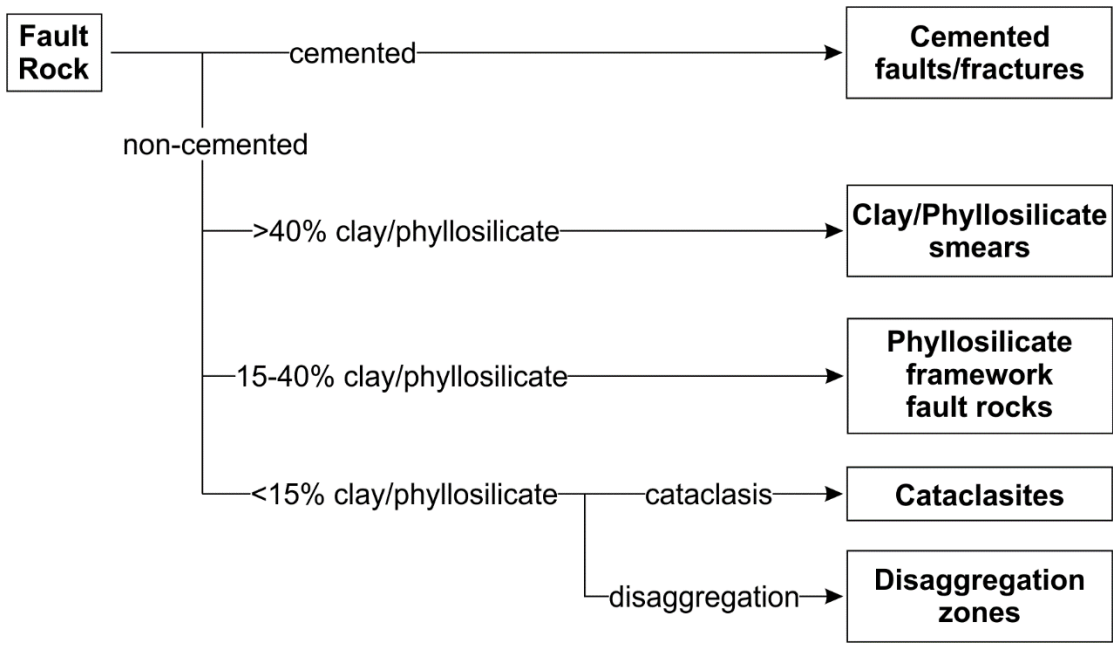
1382 **Figure 2**



1383

1384

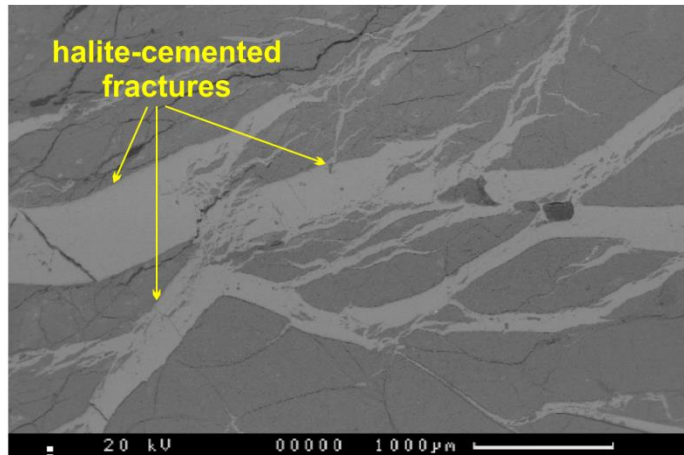
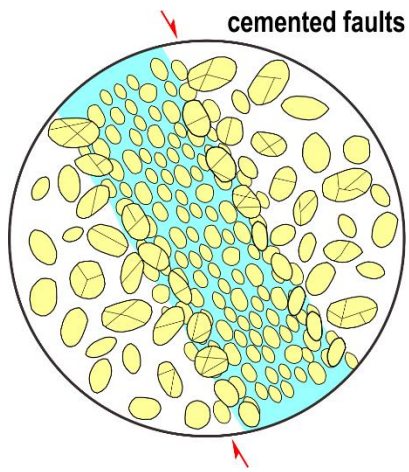
1385 **Figure 3**



1386

1387

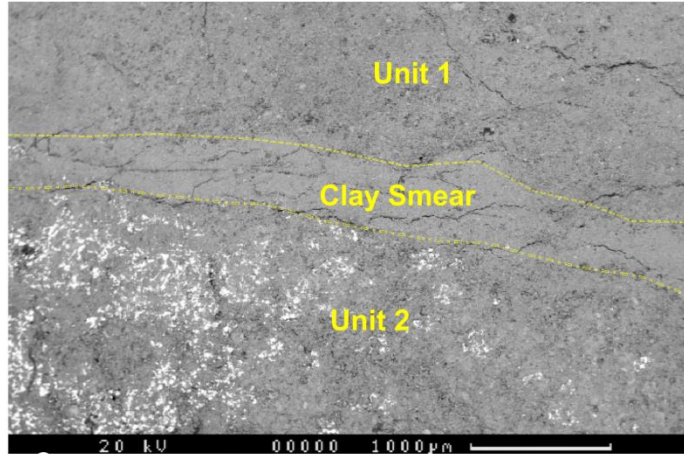
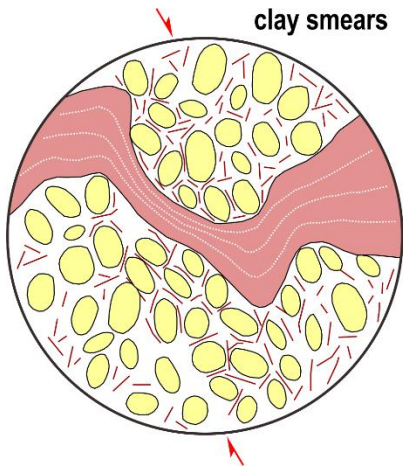
1388 **Figure 4**



1389

1390

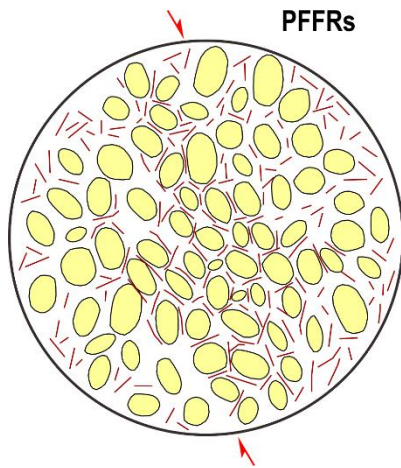
1391 **Figure 5**



1392

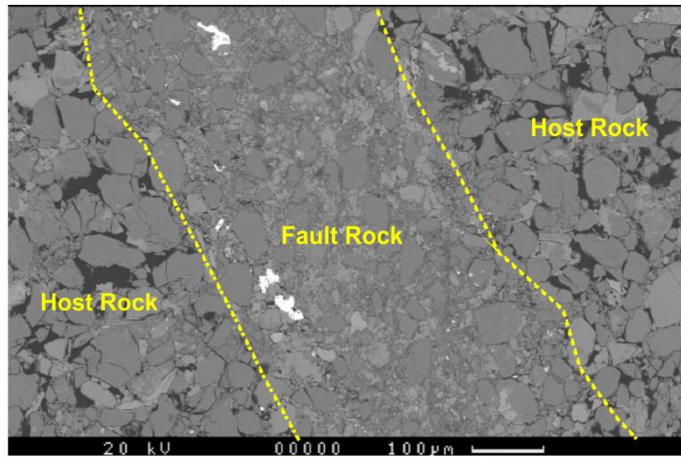
1393

1394 **Figure 6**

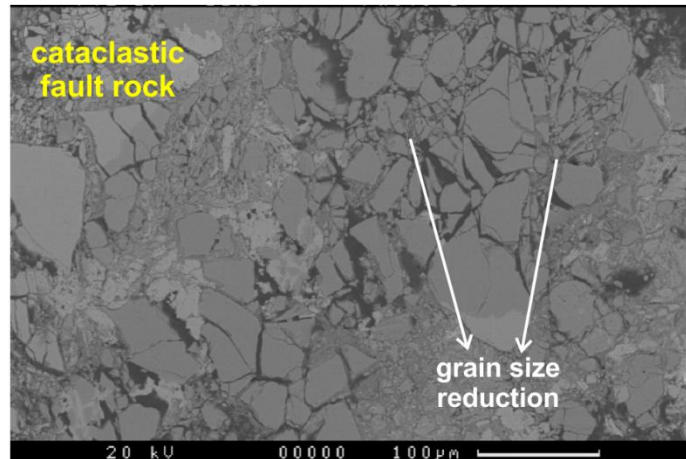
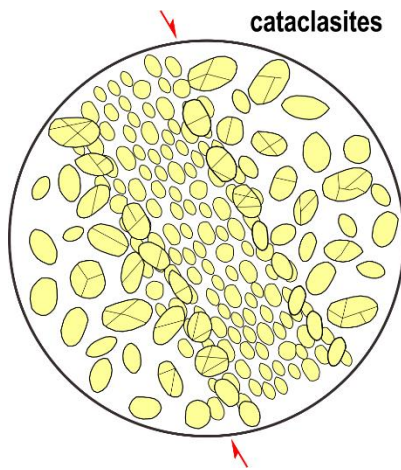


1395

1396



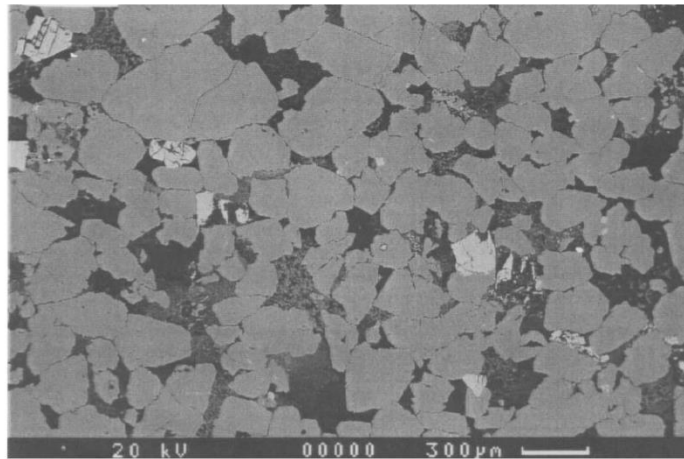
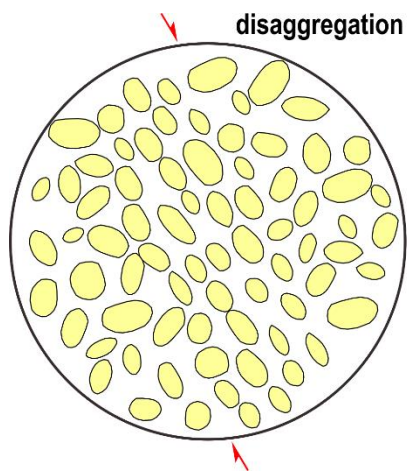
1397 **Figure 7**



1398

1399

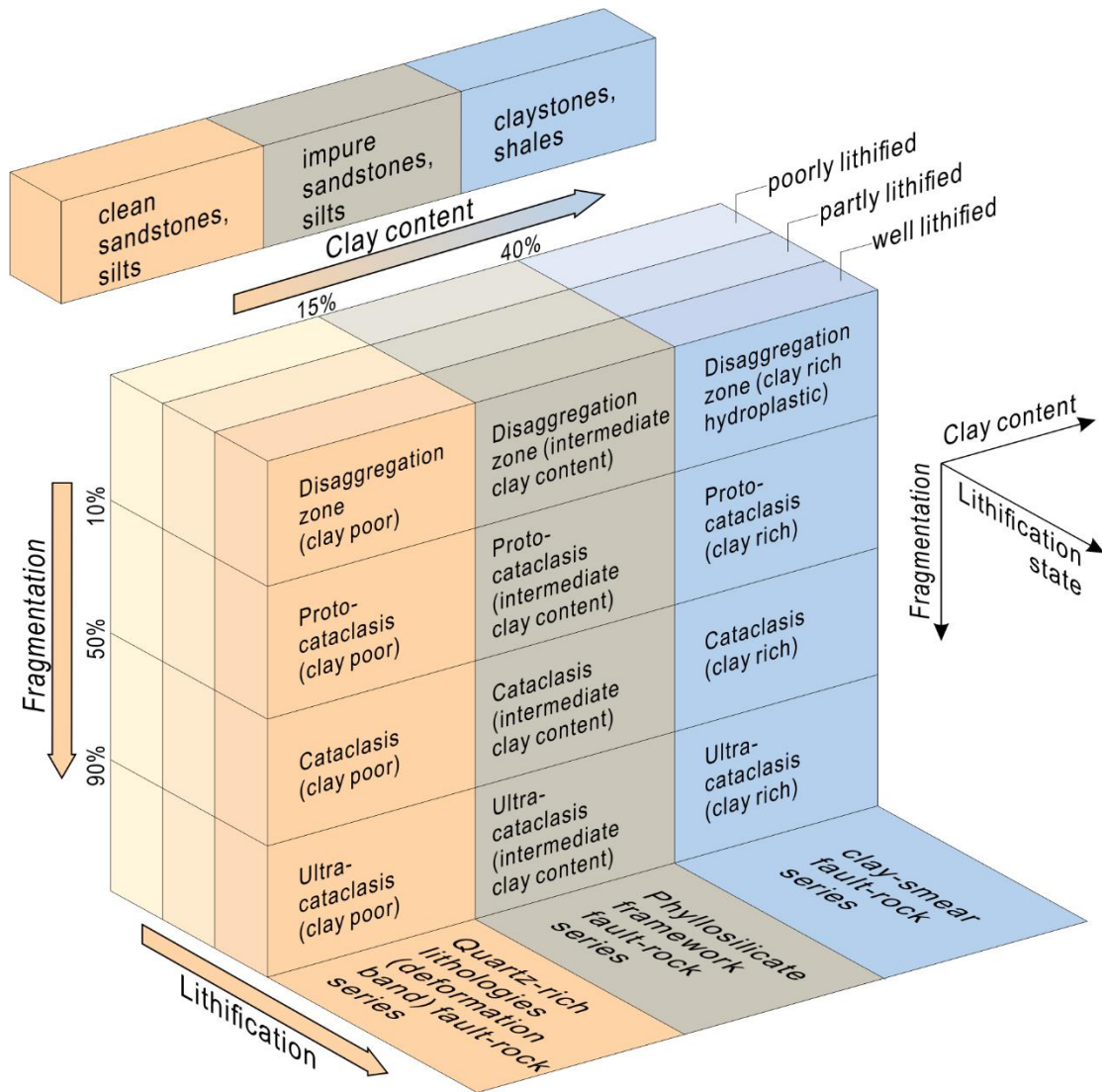
1400 **Figure 8**



1401

1402

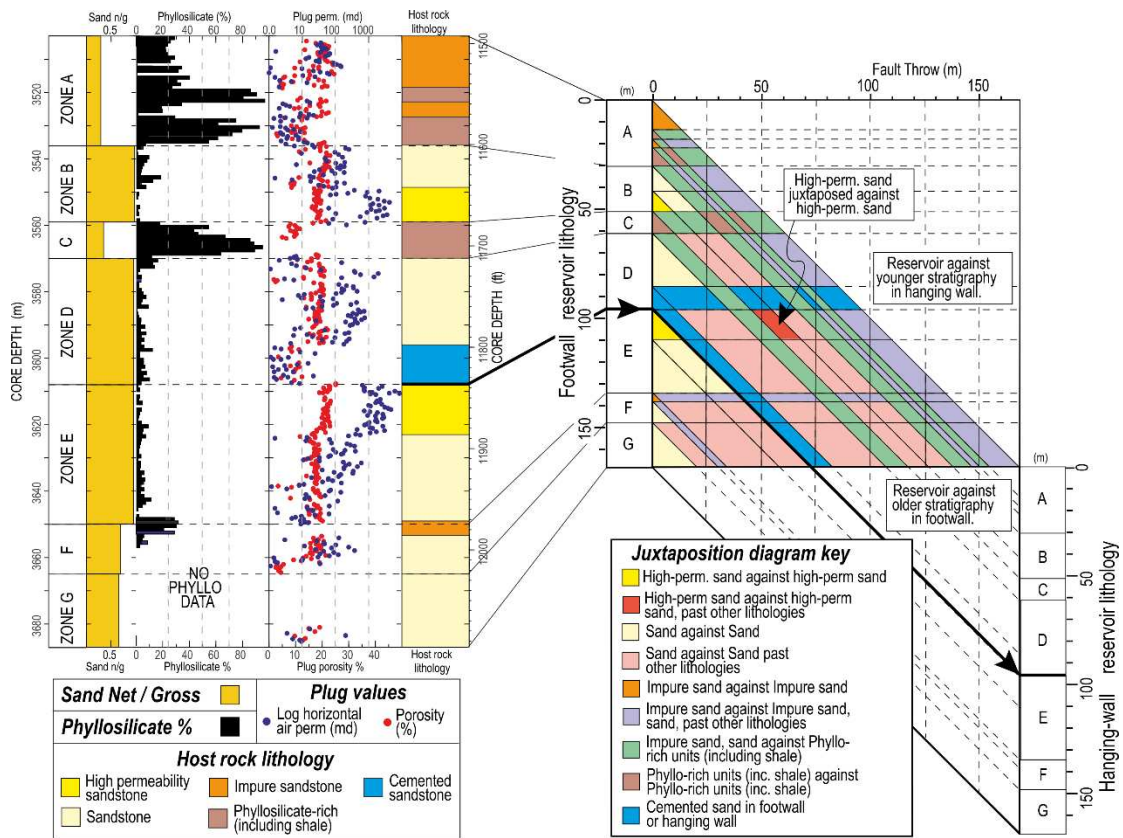
1403 **Figure 9**



1404

1405

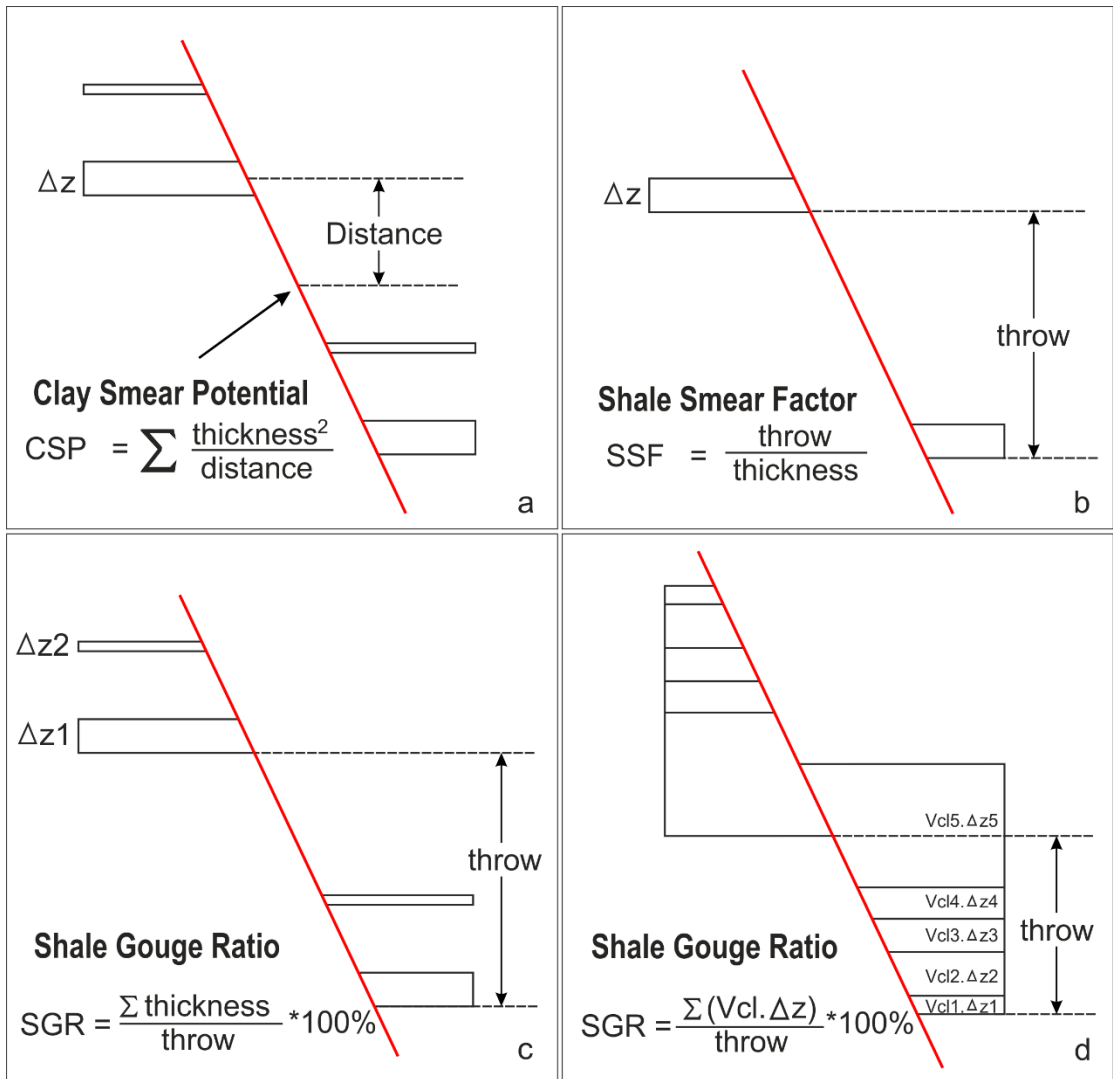
1406 **Figure 10**



1407

1408

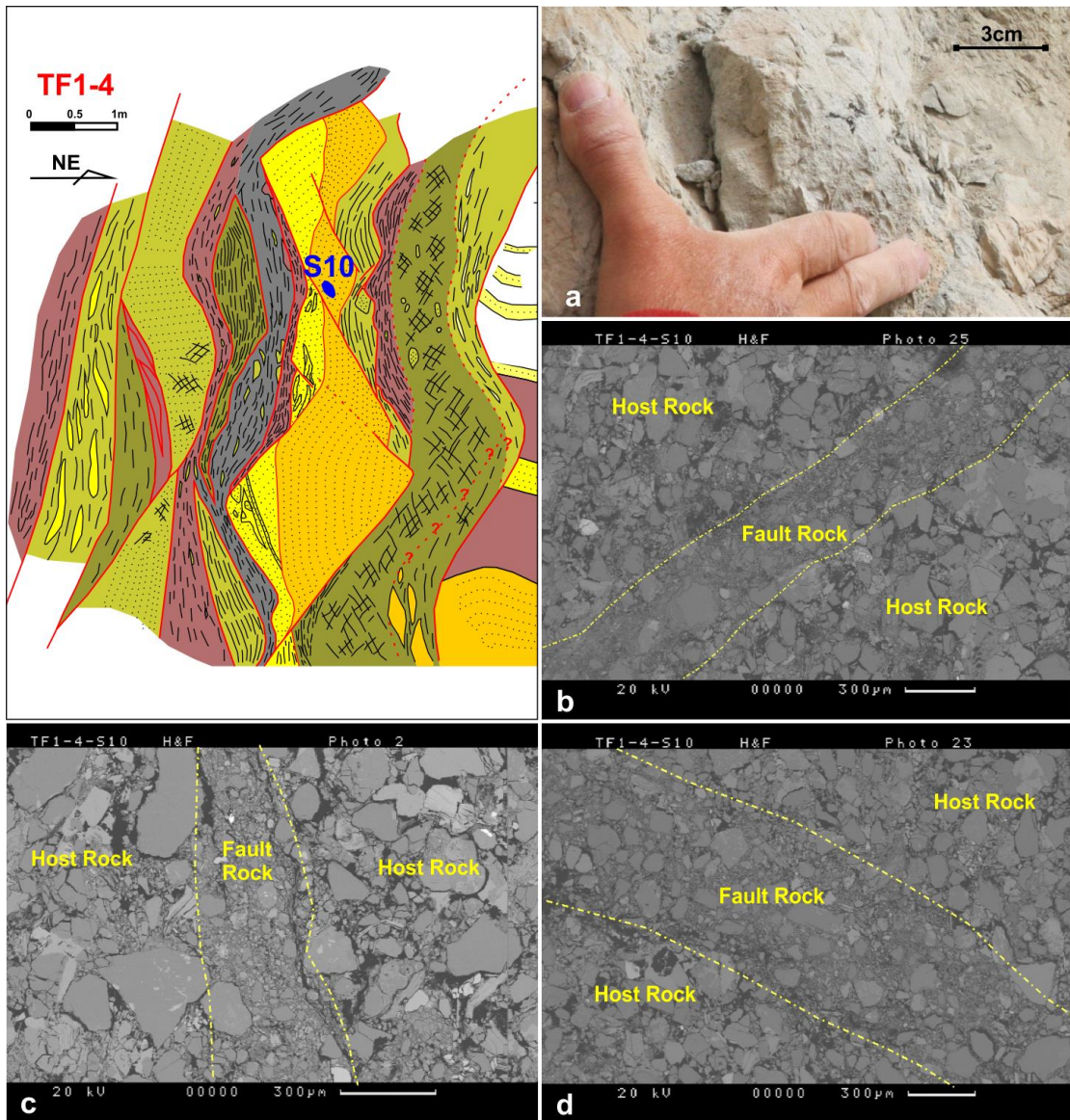
1409 **Figure 11**



1410

1411

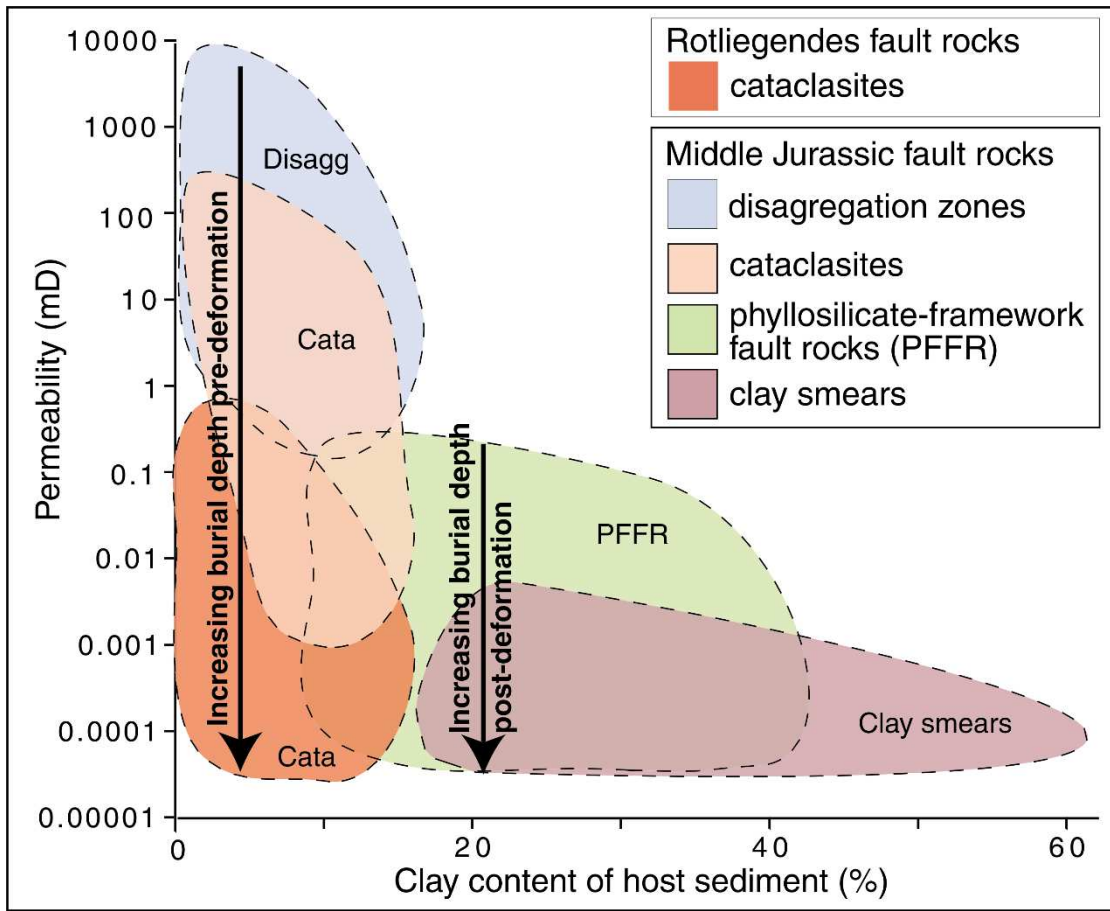
1412 **Figure 12**



1413

1414

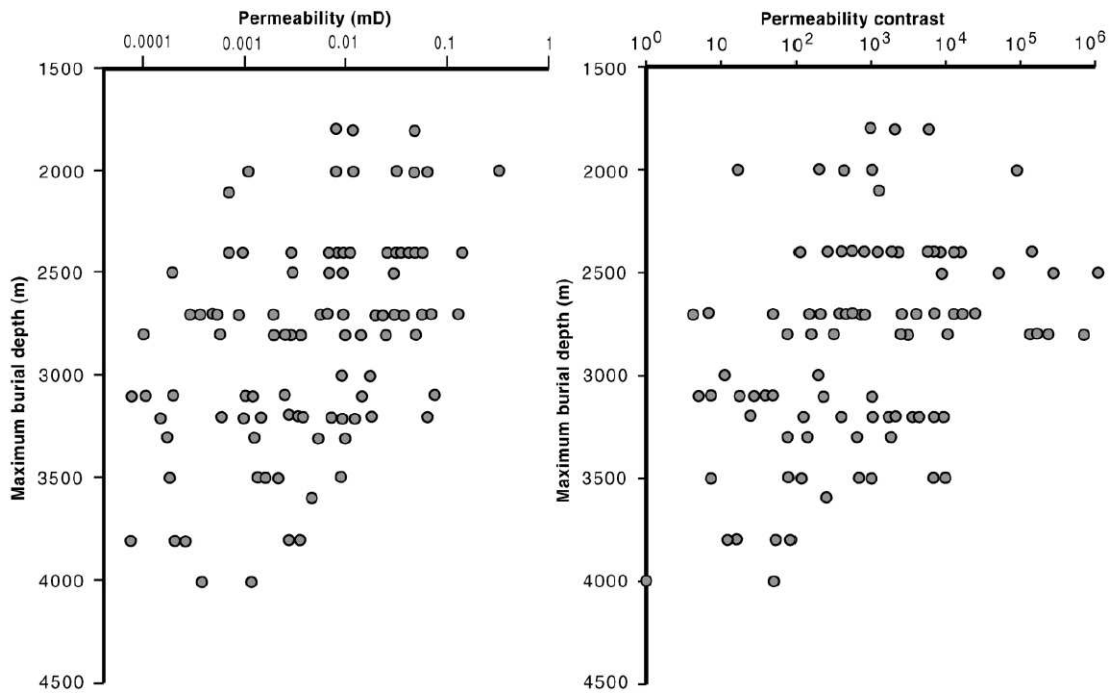
1415 **Figure 13**



1416

1417

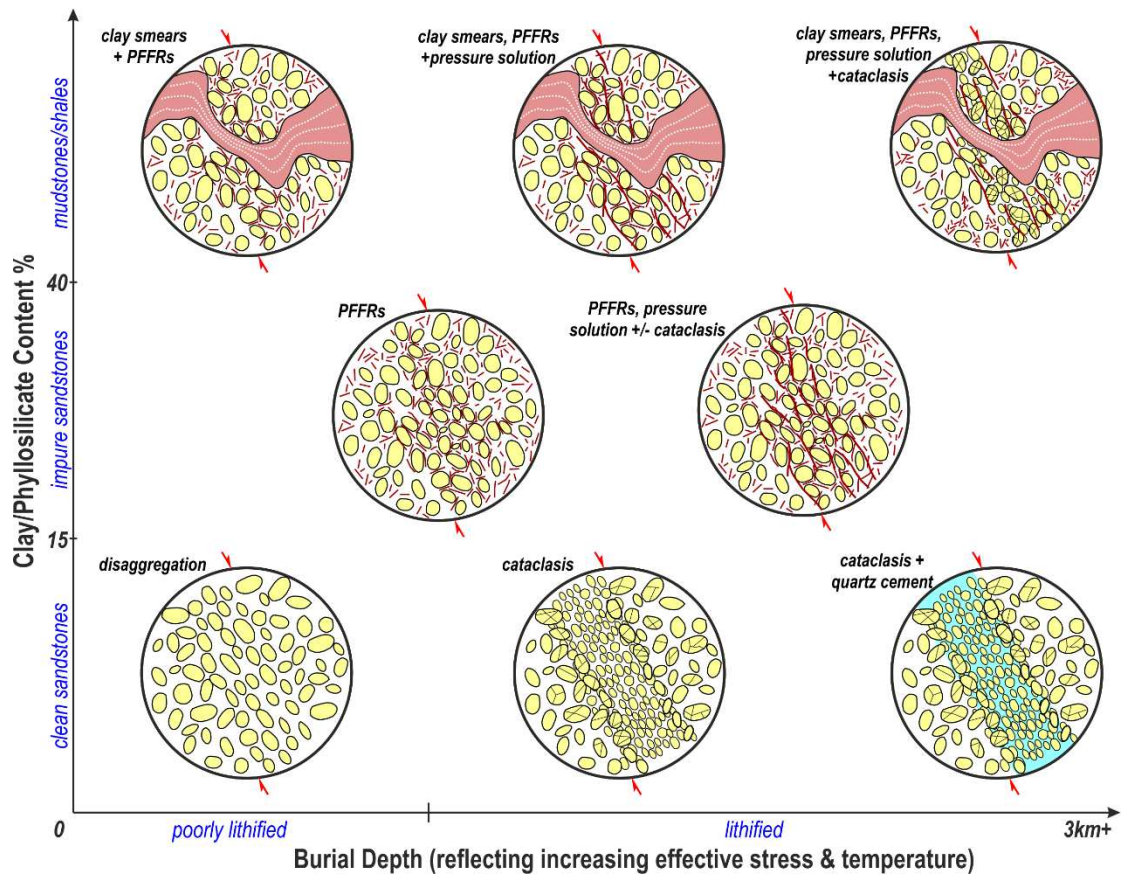
1418 **Figure 14**



1419

1420

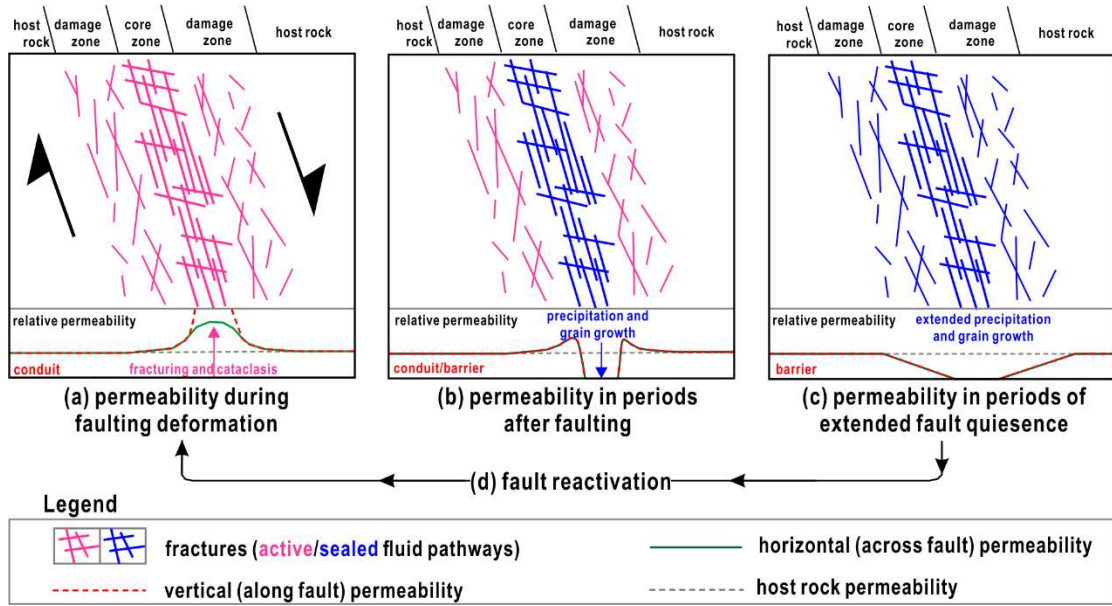
1421 **Figure 15**



1422

1423

1424 **Figure 16**



1425

1426

1427 **Table 1**

<i>fault seal classifications</i>	<i>methods</i>	<i>references</i>
	<i>Allan map</i>	<i>Allan (1989)</i>
	<i>triangle juxtaposition diagram</i>	<i>Knipe (1997)</i>
<i>juxtaposition seals</i>		<i>Bouvier et. al., (1989)</i>
	<i>clay smear indices</i>	<i>Fulljames et al., (1997)</i>
		<i>Lindsay et al., (1993)</i>
		<i>Yielding et al., (1997)</i>
		<i>e.g., Knipe, (1992)</i>
<i>fault rock seals</i>	<i>micro-structural analysis</i>	<i>Fisher and Knipe, (1998)</i>
		<i>Ottesen Ellevset et al., (1998)</i>
	<i>petrophysical assessment</i>	<i>Fisher and Knipe (2001)</i>
		<i>Tueckmantel et. al., (2010)</i>

1428

1429

1430